



**HAL**  
open science

## Geoarchaeological investigation of the Quriyat coastal plain (Oman)

Tara Beuzen-Waller, Pierre Stéphan, Kosmas Pavlopoulos, Stéphane Desruelles, Anaïs Marrast, Simon Puaud, Jessica Giraud, Éric Fouache

► **To cite this version:**

Tara Beuzen-Waller, Pierre Stéphan, Kosmas Pavlopoulos, Stéphane Desruelles, Anaïs Marrast, et al.. Geoarchaeological investigation of the Quriyat coastal plain (Oman). *Quaternary International*, 2019, 532, pp.98-115. 10.1016/j.quaint.2019.10.016 . hal-03133988

**HAL Id: hal-03133988**

**<https://hal.science/hal-03133988>**

Submitted on 1 Mar 2022

**HAL** is a multi-disciplinary open access archive for the deposit and dissemination of scientific research documents, whether they are published or not. The documents may come from teaching and research institutions in France or abroad, or from public or private research centers.

L'archive ouverte pluridisciplinaire **HAL**, est destinée au dépôt et à la diffusion de documents scientifiques de niveau recherche, publiés ou non, émanant des établissements d'enseignement et de recherche français ou étrangers, des laboratoires publics ou privés.

## Geoarchaeological investigation of the Quriyat coastal plain (Oman)

2

BEUZEN-WALLER Tara, STÉPHAN Pierre, PAVLOPOULOS Kosmas, DESRUELLES

4 Stéphane, MARRAST Anaïs, PUAUD Simon, GIRAUD Jessica, FOUACHE Éric.

### 6 **Corresponding author:**

BEUZEN-WALLER Tara, tara.beuzen@gmail.com, Faculté des lettres  
8 de Sorbonne Université, FRE ENeC 2026 / UMR ArScAn 7041, 191 rue Saint-Jacques, Paris,  
France

### 10 **List of Authors & affiliations:**

STÉPHAN Pierre, CNRS, Université de Bretagne Occidentale, UMR LETG 6554, Institut  
12 Universitaire Européen de la Mer, Plouzané, France

PAVLOPOULOS Kosmas, Département de géographie et d'aménagement, Sorbonne  
14 Université Abu Dhabi, FRE ENeC 2026, Al Reem Island, Abu Dhabi, UAE

DESRUELLES Stéphane, UFR de Géographie et Aménagement, Faculté des lettres  
16 de Sorbonne Université, FRE ENeC 2026, 191 rue Saint-Jacques, Paris, France

MARRAST Anaïs, Muséum national d'Histoire naturelle, UMR AASPE 7209, CP 56 - 57 rue  
18 Cuvier, Paris, France

PUAUD Simon, Muséum national d'Histoire naturelle, UMR HNHP 7194, 1 rue René Panhard,  
20 Paris, France

GIRAUD Jessica, Archaios / UMR ArScAn 7041, 6 rue Lacépède, Paris, France

22 FOUACHE Éric, UFR de Géographie et Aménagement, Faculté des lettres  
de Sorbonne Université, FRE ENeC 2026, 191 rue Saint-Jacques, Paris, France

24

**Keywords** : Coastal plain, Geoarchaeology, Geomorphology, Mid-Late Holocene, Overwash

26 deposits, Oman

28 **Abstract**

Due to the richness of its coastal environments, particularly lagoons and mangrove, the low-lying areas of the Omani coastline attracted settlements very early. However, the low-lying coasts are highly mobile landscapes, whose evolution is controlled by multiple factors acting at different timescales, from episodic (extreme events) to millennial timescales (gradual shoreline changes). From a geoarchaeological analysis (geomorphological mapping, archaeological survey, core drilling, and sedimentological, faunic and microfaunic analyses), this study proposes for the first time to reconstruct the strong landscape evolution of the Quriyat coastal plain landscape during the Mid-Late Holocene. Results indicate a coastal landscape dominated by large lagoons and mangroves during the mid-Holocene (5th millennium). Between 6712–6501 cal. BP and 6183–5992 cal. BP, an extreme wave event identified as a tsunami, is registered in the southern part of the coast. Between 4223–3984 cal. BP and 4150–3981 cal. BP, lagoons were quickly clogging over more than 3.5 km in favour of the development of sebkhas or dune fields. We suggest this rapid evolution is related to erosional crises linked to the setting up of arid conditions in this part of the Omani coast. The production of several sea-level index points shows a great stability of the relative sea-level over the last 6.000 years cal. BP and point out the predominant role of sedimentary infilling in the coastline evolution of Quriyat. The high sedimentation rates, added to the exposure of coastal hazards, partially explains the relatively low density of archaeological sites found in the Quriyat coastal plain, despite the presence of major shell-midden (Khor Milk I and II), which attest the old attractiveness of this sector. From geoarchaeological and taphonomic points of view, the Quriyat area is considered as having non-favourable conditions for the preservation of archaeological remains.

## 1. Introduction

54

### 1.1. The long-term interactions between the Omani coastal environment and societies

56           The seafront of the Sultanate of Oman currently concentrates settlements and economic  
activity. The passage of tropical cyclones Gonu and Phet along the Sultanate of Oman coasts  
58 in year 2007 and 2010, respectively (Fritz *et al.*, 2010; Haggag and Badry, 2012), revealed the  
high vulnerability of low-lying urbanized areas located at the mouth of large *wadis* (local term  
60 for watercourse) (Azaz, 2010), where coastal flooding and flash floods are most significant. In  
the coastal areas of Oman, flooding hazards are linked to two phenomena: 1) storm surges  
62 generated by tropical cyclones from the northern Indian Ocean (Murty and El Sabh, 1984) 2)  
tsunamis caused either by underwater landslides along Owen's ride (Rodriguez *et al.*, 2013), or  
64 by seismic activity along the Makran subduction zone (El Hussain *et al.*, 2016; Hoffman *et al.*,  
2013a). As a result, the Omani coast is particularly exposed to meteo-oceanic and seismic  
66 hazards, which can abruptly transform coastal landscapes. Little is known about the frequency  
and intensity of these events on a long-term scale (El-Hussain I. *et al.*, 2016), and their influence  
68 in the human settlement patterns.

          The long-term interactions between settlement patterns and the Omani coastal  
70 environments have only recently been investigated, notably by the geoarchaeological research  
conducted by the Joint Hadd Project (dir. Tosi M. and Cleuziou S.), by the Ja'alan-Dhoffar  
72 French Mission (dir. Charpentier V.), as well as today by the ANR NeoArabia project (dir.  
Berger J.-F) and the GUTech project "Coastline of Oman (dir. Hoffmann G.). These projects  
74 highlight that since prehistoric periods, the Omani coasts (Fig. 1) have attracted populations for  
various reasons (Fig. 2). During the Neolithic period, from ca 8000-5000 BP, the seashores of  
76 Oman presented attractive environments (Tengberg, 2005), notably lagoon and mangrove for  
their marine (fish, molluscs, crustaceans) and terrestrial (wood) resources. Berger *et al.* (2013)

78 demonstrated that the interactions between Neolithic populations and their coastal  
environments fit with the larger extension of paleo-mangroves during the Holocene humid  
80 period (ca 10500 to 5000 BP) (Parker *et al.*, 2006; Fleitmann and Matter, 2009). The influence  
of monsoon rains (Berger *et al.*, 2013) has favoured the development of tropical mangroves,  
82 such as *Rhizophora mucronate*. This species is now absent from the Omani coasts (Lézine *et*  
*al.*, 2002; Lézine *et al.*, 2017) in favour of *Avicennia marina*, more resistant to high salinity  
84 levels. The link between Neolithic groups and coastal environments is testified by numerous  
shell middens distributed along the Omani coast (Biagi, 1994), particularly well registered in  
86 the area between Muscat and Masirah. Archaeological remains from the Neolithic period are  
found in the interior of Oman to a lesser extent, and mainly consist of surface lithics spread.  
88 During the Bronze Age period (ca. 5200-3300 BP), the emergence of the Oasian way of life  
(agriculture, long-term occupation and solid construction) caused a significant change in  
90 settlement distribution (Beuzen-Waller *et al.*, 2018), as the Omani mountains and piedmont  
started to be populated. This evolution in the way of life, which took place from the Neolithic  
92 to the Bronze Age period, was sometimes interpreted as an adaptation to aridification at the end  
of the Holocene humid period (Lézine *et al.*, 2002), and/or as a response to the clogging of  
94 lagoonal environment, and the reduction of mangrove forest (Berger *et al.*, 2005).

Despite environmental issues, some strategic sites of the coastal area, such as Ras al-  
96 Jinz (Fig. 2), kept economic attractiveness during the Bronze Age, as they show evidence of  
exchange with the Indus Valley and the Middle East. Moreover, an Early Bronze Age site  
98 (between 5050 and 4450 cal. BP) of Ras al-Hadd, called “HD-6” (Azzara, 2013), presents the  
first evidence of coastal hazard exposure (Fig. 1). The Early Bronze Age stratigraphy was cut  
100 by a shell debris level dating back to 4450 cal. BP, and located at an elevation of +2.5 m asl  
(above sea-level). Hoffmann *et al.* (2015) suggested the tsunamigenic origins of this layer. The  
102 latter is comprised between two occupation phases of the Bronze Age, which testifies to the

fact HD-6 was reoccupied, even though it was exposed to flooding. During the Iron Age  
104 (between 3250-2250 cal. BP), despite an arid climate like the present one (Fleitmann *et al.*,  
2007, Parker *et al.*, 2016) the production and exchange of copper reached a peak. The  
106 domestication of camels (Almathen F., *et al.* 2016) and the development of the *falaj* system  
(underground water supply) (Charbonnier J., 2015) facilitated the consolidation of commercial  
108 roads in the interior of Oman, as well as the occupation or crossing of constraining  
environments.

110

## **1.2. The use of geoarchaeology to study the interactions between archaeological site 112 localisation and environmental evolution in the eastern coast of Oman**

From the Neolithic to the Iron Age, the coastal area shows important changes that might  
114 have influenced past societies in their strategies of settlement. Yet, geomorphologic dynamics  
of the coastal areas and of their evolution might also have influenced the preservation,  
116 destruction or burying of archaeological sites, and geoarchaeological research can help to  
investigate the taphonomic potential of some areas.

118 In the area between Muscat and Masirah, geoarchaeological studies (Fig. 1 and Fig.2)  
highlighted a variety of factors that had influenced the gradual evolution of landscapes and  
120 coastal resources since the Middle Holocene. Those factors are : 1) the relative influence of  
relative sea-level variations: the slowdown and steadying of the eustatic sea-level around ca.  
122 4000 BP (Hallmann, 2018; Lambeck, 2014; Lambeck, 1996); 2) the regional or local tectonic  
uplift (Kusky *et al.*, 2005; Hoffmann *et al.*, 2013a; Moraetis *et al.*, 2018; Falkenroth *et al.*,  
124 2019); 3) the climate aridification and its hydrological consequences: the scarcity of surface  
runoffs, and the reduction of freshwater inputs to lagoons (Fleitmann *et al.*, 2007; Berger *et al.*,  
126 2012; Berger *et al.*, 2013); 4) the importance of continental winds and river dynamics in the  
progradation of coastal areas, and in the clogging of lagoons (Sanlaville and Dalongeville,

128 2005); 5) the importance of anthropogenic factors such as intensive mangrove exploitation  
(Tengberg, 2005), which, in some sectors, would be the main force behind mangrove loss.

130 The coastal plain of Quriyat is located between Muscat and Sur (Fig. 1). It is one of the  
only coastal plains where prograded landforms can be observed, in this case the delta of Wadi  
132 Dayqah, in the southern part of the plain. The northern part of the plain is occupied by a small  
mangrove, a lagoon and a sebkha. Despite a geographical configuration similar to other coastal  
134 plains rich in archaeological remains from the Neolithic and Bronze age period (e.g. Muscat  
and Ja'alan), Quriyat shows only four shell middens, and a few rare tombs dating back to the  
136 Early Bronze Age (22 in total, Fouache *et al.*, 2017), much less significant than the  
approximately 3000 cairns discovered in the Ja'alan area (Giraud, 2005).

138 In this article, we aim to question the lack of archaeological sites through the  
reconstitution of the environment around Quriyat during the Mid-Late Holocene, as well as  
140 through an identification of taphonomic factors that may have biased the representativeness of  
archaeological sites in the low-lying coastal area. What kind of environment stood around the  
142 Quriyat coastal plain during the Neolithic and Early Bronze Age? Were its resources attractive  
during prehistoric and protohistoric periods? What kind of dynamic processes shaped the plain  
144 during the Mid-Late Holocene, and were they conducive to the preservation of archaeological  
sites?

146

## 2. Regional setting

148

### 2.1. Geology and topography

150 The coastal plain of Quriyat is located on the eastern coast of Oman (Fig. 1), in the  
northeast termination of the Hajar Mountains chain. The rocky substrate is mainly composed  
152 of carbonate formations dating from the end of the Paleocene to the beginning of the Eocene



(Le Metour *et al.*, 1983). The reliefs surrounding the coastal plain are made of alternating series  
154 of marl limestone and dolomitic, arranged on different levels. Between Muscat and Masirah,  
uplift dynamics are visible in several specific morphological features, which include twelve  
156 generations of marine terraces (Wyns *et al.*, 1992; Falkenroth *et al.*, 2019). Between Quriyat  
and Sur, the highest marine terraces reach +500 m asl, and date back to the Miocene (Wyns *et*  
158 *al.*, 1992; Hoffmann *et al.*, 2019). In the coastal area south of Quriyat, between Bimmah and  
Fins, the lowest terrace levels are depositional. These landforms are not visible at Quriyat,  
160 where only erosional terraces, up to +50 m asl, are connected to the coastal plain through very  
steep slopes. In contrast to other parts of the Omani coast, generally characterized by uplift  
162 (Moraetis *et al.*, 2018), the coastal plain of Quriyat is built on a graben (Fig. 3), partly linked to  
the presence of NW-SE orientation faults along Hayl al Ghaf, and W-E along the Jebel Satari  
164 (Wyns *et al.*, 1992) (Fig.1 and Fig.3). The northern part of the plain presents a less pronounced  
subsidence, as the highly indented morphology of the rocky coasts north of the Jebel Satari  
166 suggest (Hoffmann *et al.*, 2013b).

Framed in medium altitude plateau (Jebel Satari, Jebel Qashru, and Hayl al Ghaf, Fig.1  
168 and Fig.3) comprised between +200 and +600 m asl, the plain extends from north to south over  
14 km, and from west to east over 4.5 km. Elevation in the plain slowly decreases towards the  
170 sea, except for areas where dunes are located. The highest observed dunes reach +15 m asl.  
Three wadis feed the plain (Fig. 1d). In the northern part of the plain, Wadi Miglas ends with a  
172 small lagoon and a mangrove swamp. In the central part, Wadi Qahmah, which now has a  
completely artificial stream, generally sinks into the sands, and only very exceptionally reaches  
174 the sea. Wadi Qahmah leans against a vast, coastal sebkha that joins the open lagoon of Quriyat.  
The sebkha perimeters are covered with fine silts, locally called “khabras”, on which traditional  
176 oases have developed. The southern part of the plain is crossed by Wadi Daqyah, whose lobed  
delta is, by far, the most developed and prograded coastal form on the east coast of Oman. Wadi

178 Dayqah's distributaries extend in a rather homogeneous fan shape. They are separated by pebble  
stream bars covered with aeolian sand, reaching an elevation of +2.5 m asl. The distributaries  
180 outlet ends with either open or closed sand spits that are strongly disrupted, or even destroyed  
during every major meteorological event. With a catchment area extending 1 700 km<sup>2</sup>, Wadi  
182 Dayqah is one of the most active wadis in the Sultanate of Oman and one of the rare perennial  
watercourse, experiencing flush floods during severe storms. Over the last fifteen years, this  
184 wadi was subject to significant artificialization to prevent extreme flood events. The two  
cyclones Gonu and Phet caused catastrophic floods that lead to significant material damages  
186 and human casualties in the Quriyat area (Fritz *et al.*, 2010; Haggag and Badry, 2012). In  
response to the flood impacts, the streams of Wadi Dayqah were heavily artificialized to protect  
188 the buildings (see Google Earth images from 2010 to 2018). The dikes greatly narrowed and  
simplified the geometry of the Wadi Dayqah floodplain. Several branches of the delta, including  
190 Wadi Munaysif, were disconnected. This high reactivity to extreme events ranks the wadis (and  
their floodplain) among the most active and mobile geomorphological units on the Quriyat  
192 Plain.

## 194 **2.2. Climate and environment**

Like most places in the Arabian Peninsula, Quriyat is dominated by desert  
196 environments, and arid climate. The average annual temperature is 28.3°C, and the average  
annual rainfall is 89 mm (averages calculated on a 24-year base, data from the Directorate  
198 General of Meteorology, Oman). According to the Köppen-Geiger classification, Quriyat falls  
into the hot desert climates (BWh). The upstream part of the wadis feeding the Quriyat coastal  
200 plain has its source in the range of the Hajar Mountains, and can reach 1000-1100 m asl (data  
from the Directorate General of Meteorology, Oman). These areas benefit from heavier  
202 orographic rains, like in Hayl al Kabir – the upstream part of Wadi Dayqah's watershed –,

where the average annual rainfall is 139 mm. In any case, winter rainfalls are sporadic, and  
204 highly variable in time and space. Hence, wadis occur intermittently, are characterized by  
patterns of torrential flow, and they exhibit high variability in the size and frequency of floods.  
206 In the area of Quriyat, severe flash flood events mainly occurred during tropical cyclones.  
Erosional processes are eased by very low soil development, often limited to regosol. Scarce  
208 vegetation and bedrock exposure allow an active, physical weathering that supplies an abundant  
bedload and suspended sediment load. Sediment transport mainly occurred during major floods.  
210 Alluvial deposits from the wadis have braided channel facies, and are dominated by coarse-  
grained sediments in the proximal zone of the floodplain. Finer sediment were found in the  
212 distal part of the floodplain, and in an abandoned channel. Aeolian processes are also very  
active, and deflation often carries out finer sediments when the latter remain dry or exposed for  
214 a long time.

In Oman, the vegetation better develops in low-lying coastal areas, where halophytic vegetation  
216 and mangrove can grow, especially in sheltered places or lagoons. The current mangrove is  
dominated by the Grey Mangrove (*Avicennia marina*), which can be observed in the northern  
218 part of the Quriyat coastal plain. The tide regime is mesotidal, as the maximum tidal range in  
Quriyat is 3 m. Incident waves mainly come from the north-east from September to July, and  
220 from the south during the summer. The main longshore drift is oriented from south to north.

### 222 **2.3. Archaeological sites**

In Quriyat, several Neolithic shell clusters have been identified in surveys (carried out  
224 in the 1980s and as part of this study) (Fig. 2): three of them were identified along Wadi Miglas  
(Uerpmann, 1992), and two particularly well developed shell middens, namely the Khor Milk  
226 I and Khor Milk II sites (Fig. 2 and Fig.3). The main cluster, Khor Milk I, is 10 m high, 290 m  
long and 120 m wide. Several artefacts, such as hooks and net weights were discovered on the

228 surface, and attest to the exploitation of fishery resources (Phillips and Wilkinson, 1979).  
Except for the major site of Khor Milk I, the coastal plain of Quriyat is relatively poor in  
230 archaeological remains. Despite Bronze Age cairns being visible on Hayl al Ghaf, no Iron Age  
site has been discovered so far. Given the high attractiveness of the coastal plain in terms of its  
232 environmental resources and strategic position, the relative lack of sites is a real curiosity (Fig.  
2) that we investigate in this study.

234

### 3. Material and methods

236

To identify the multiple dynamics at work in the shaping of the Quriyat plain from the mid-  
238 Holocene, we applied a multidisciplinary approach, including geomorphological,  
archaeological, sedimentological, malacological and micropalaeontological studies.

240

#### 3.1. Geomorphological mapping: integration of published data and analysis of satellite 242 imagery

The Quriyat plain was the subject of two geoarchaeological surveys in the late 1990s,  
244 one involving Paulo Biagi and Claudio Vita-Finzi (Biagi, 1994), and the other led by Christian  
Hannss and Margarethe Uerpmann (Hannss, 1999). Both surveys led to the mapping of several  
246 sectors, notably the mouth of Wadi Munaysif, and the lower reaches of Wadi Miglas (Hannss,  
1999). The Quriyat area is included in two geological maps, one at 1:100 000 (Quriyat sheet:  
248 Le Métour, 1983), the other at 1:250 000 (Muscat sheet: Le Métour, 1992). These documents  
were integrated into a GIS using ArcGIS software, and georeferenced in WGS 84 UTM 40 N.  
250 We used Google Earth images from before 2006 (before Cyclone Gonu in June 2007), and after  
2011 (after Cyclone Phet in June 2010), to complete these mapping elements, and to identify  
252 geomorphological units, either active or disrupted during severe meteo-oceanic events. Finally,

field observations helped us to specify the sedimentary nature of the geomorphological units,  
254 to update the mapping, and specify the boundaries of some units. The altimetric data (Digital  
Elevation Model) was extracted from the ASTER database (Advanced Spaceborne Thermal  
256 Emission and Reflection). The synthesis of these operations, as well as additional geo-  
archaeological surveys (Fouache *et al.*, 2017), enabled us to produce a geomorphological map,  
258 and to precisely understand the organization and composition of the various surface formations  
of the Quriyat coastal plain (Fig. 3).

260

### 3.2. Core drilling and topographic survey

262 Core drilling were conducted to determine the nature of sedimentary deposits, and to  
date the infilling of the coastal plain. We selected three sampling areas: the Quriyat sebkha, the  
264 dune field, and the delta of Wadi Dayqah (fig. 1 and Fig. 3). Six cores were drilled in the Quriyat  
sebkha, and two at the boundaries of the dune field, using a Cobra-type mechanical vibracoring  
266 (cores are named QU, see Fig.3 and Fig. 4). They were supplemented by three trenches (named  
S), and by the study of three ditches, exposed by a digging pipe (named QT, see Fig. 3 and fig  
268 5). We placed every stratigraphic series within a precise altimetric frame by conducting  
topographic surveys with a Trimble DGPS in RTK mode. Each DGPS measurements was  
270 calibrated from the mid-tide level, using the geodesic marker located at Quriyat harbour. The  
reference value for the mean-tide level is provided by the Oman National Hydrographic Book  
272 (ONHB, 2014).

### 274 3.3 Stratigraphic and morpho-sedimentary analysis

In total, we studied 47 meters of cores and sections in the LETG laboratory (in Brest,  
276 France), and in the geochemistry laboratory of the National Museum of Natural History (Paris,  
France). Each sedimentary deposit was identified and the morpho-sedimentary units were

278 described. The study of sedimentary facies was completed through particle size measurements,  
using a Malvern Mastersizer 2000 laser particle size analyser. These measurements were made  
280 every 5 cm on the QU4 core, every 10 cm on the QT3 section, and every 5 cm on the shell  
deposits in QT3.

282 On core QU4, sediments were analysed after a hydrogen peroxide treatment, and  
sampled with suspended sediments kept in sodium hexametaphosphate solution. The QT3  
284 sediments were subjected to three microgranulometric measurements. The first measured  
sediments were suspended in sodium hexametaphosphate. In order to clear peat deposits, the  
286 second measurements were carried out after the removal of organic matter with hydrogen  
peroxide in solution. The third measurements were realized after the removal of carbonates  
288 (hydrochloric acid 47%) in order to remove shell fragments (Founier *et al.*, 2012). In addition,  
the percentage of coarse elements was performed by weight (total sample weight, and weight  
290 of elements less than 2 mm in diameter).

### 292 **3.4 Study of malacofauna and micro-fauna**

The study of macro-faunal and micro-faunal remains was used to identify marine units,  
294 and to characterize lagoon units (Fig.6). Malacological remains were identified in several cores,  
including QU4, QU6, QU7 and QT3, and were used as bioindicators to characterize subtidal,  
296 intertidal, and supratidal environments. Systematic identification was made in the shell levels  
related to marine submersion in order to discriminate tsunamite or tempestite deposits (Puga-  
298 Bernabéu and Aguirre, 2017).

On the other hand, foraminifera were identified and counted in a detailed, systematic study  
300 (extraction every 5 cm) of the QU4 core, and of the QT3 ditch (every 10 cm over the entire cut,  
and every 5 cm at the shell deposit). The extraction of foraminifera was carried out from a wet  
302 sieving sediment, after washing residues of the fraction between 500 and 63  $\mu\text{m}$ , as suggested

both by Murray (1991), and Horton and Edwards (2006). The wet sieving sediment was treated  
304 with trichloroethylene in order to sample the floating foraminifera. Species identification was  
based on observations by Pilarczyk *et al.* (2011), who sampled and analysed the surface  
306 distribution of foraminiferous assemblages in the Sur lagoon. Foraminifera from the Makran  
tsunami deposits in the Sur lagoon, were also studied with the objective of being used as a  
308 reference for the recognition of ancient flooding phenomena (Pilarczyk *et al.*, 2011; Pilarczyk  
and Reinhardt, 2012). Our analyses focused on counting and enumerating foraminifera, and the  
310 assemblages obtained were interpreted according to the reference bio-facies of the Sur lagoon.

### 312 **3.5. Radiocarbon dating**

Radiocarbon dating was carried out on plant remains present in peaty levels or on coals.  
314 A total of 6 samples were dated by the Beta Analytics laboratory (Table 1). Conventional ages  
were recalibrated using Calib 7.0 software (Stuiver and Reimer, 1993), and the IntCal13  
316 calibration curve (Reimer *et al.*, 2013). The dates extracted from the bibliography, and reused  
to produce synthesis figures as well as the calculation of sea-level index points, were also  
318 calibrated with the aforementioned software. The reservoir effect was considered for the shells  
using the Marine13 calibration curve, with a delta R of 278 estimated from the Marine reservoir  
320 correction database (Reimer *et al.*, 2013) (Table 1).

### 322 **3.6. Relative sea-level reconstruction**

Sedimentological analyses, calibrated radiocarbon dates, and topographic data were  
324 used to reconstruct the Holocene relative sea-levels at Quriyat. Data processing was based on  
the "sea-level index points" method established by Hijma *et al.* (2015), which is based on the  
326 compilation of data relating to an old sea-level, and repositioned with respect to the local mid-  
tide level. Uncertainties relating to 1/ the altimetric position of the sampled data, 2/ the dating

328 methods used, 3/ the paleoenvironmental significance of the indicator studied, and 4/ the  
amplitude of the tide, are compiled and considered in the calculation of the "sea-level index  
330 points" (see table in appendices). The proposed, relative sea-level for each sample is presented  
as an indicative range, compiling both the uncertainties related to the vertical position of the  
332 samples, and the uncertainties related to dating. Corrections considering the old tidal range were  
included.

334

## 4. Results

336

### 4.1. An asymmetrical distribution of superficial sediments

338 Geomorphological mapping enabled the characterization of surficial formations that  
currently compose the Quriyat coastal plain (Fig. 3). A clear asymmetry in the preservation or  
340 fossilization of river palaeoforms was identified. It appears that the alluvial terraces of Wadi  
Miglas are much better developed and preserved than those of Wadi Qahmah and Wadi Dayqah.

342 In the northern part of the coastal plain, four levels of alluvial terraces (T1-T2-T3-T4)  
were identified along the Wadi Miglas. T1 is the most ancient one and reach an elevation of  
344 +10 m above the present wadi bed level (above river level: arl). T2 (+7/6 m arl) was preserved  
only on the upper stream of Wadi Miglas. Levels T2 and T3 (relatively dated to the late  
346 Pleistocene) consist of highly eroded terrasses distributed near the slopes and at the apex of the  
alluvial cones of Wadi Satari. The T3 level reached +4 m arl and consisted of cemented coarse  
348 pebbles. It was largely replaced by the T4 level (Fig. 3), averaging 1.5 m in height, and  
occupying a large part of the floodplain. The stratigraphy of the T4 level characterized deposits  
350 of a braided channel, with cross-stratified boulders/pebbles. By relative dating, Hannss (1991)  
linked the T4 construction period to the Holocene climatic Optimum, which ranges from about  
352 9000 BP to 5500 BP (Fleitmann *et al.*, 2007). The role of eustatic or tectonic factors in the



incision was not mentioned. The alluvial level (called "unstable banks" in Fig. 3) consists of  
354 sandy and cobble banks that are poorly developed and vegetated. They can be mobilized during  
floods. The current floodplain is characterized by a braided stream incised in the T4 terrace  
356 level that reached between +2 m arl and +2.5 m arl.

In Wadi Qahmah, the determination of terrace levels was not possible, as the widespread  
358 levelling of the alluvial cone was used for building purposes. Along Wadi Dayqah, ancient  
alluvial terraces were less visible, and T4 was found as an interfluvium between the various  
360 distributaries of the Wadi Dayqah delta.

Supplemented by remote sensing data (satellite images dated from 23/11/2002 to  
362 07/01/2014), the geomorphological study indicates a great stability of the dunes field during  
the period 2002-2014. The transverse dunes kept a northeast-trending wind slope (wind coming  
364 from the sea), and a similar geometry before and after the two Gonu and Phet storms, despite  
intense winds being deployed during these cyclonic events.

366

#### **4.2. General stratigraphy of the coastal plain deposits**

368

The sediment sequence in the inner part of the Quriyat coastal plain is composed of six  
370 main stratigraphic units. From base to top, we identified (Fig. 7): SU1: grey, coarse shelly sands,  
SU2: fine blue-green sands with shells, SU3: a silty peat rich in organic macro-remains, SU4:  
372 silty sands containing various plant remains and shell debris, SU5: fine gleyed hydromorphic  
sands; SU6: finely bedded yellowish sands, SU7: medium to coarse aeolian sands. Due to the  
374 large distances between each of the investigated sampling areas (6.4 km separate the Wadi  
Dayqah's area from the sebkha), we separately present the results of our stratigraphic analysis,  
376 from south (Wadi Dayqah's area) to north (the sebkha area). On average, the distance between  
the sampled areas and the current shoreline is 3 km.

378

#### 4.2.1. Wadi Dayqah's area

380

The observations and sediment samplings realized along the trenches QT1 to QT3, indicate the base of the sediment sequence is composed of greyish/blueish sand unit (Fig. 7). Along the trench QT3, this deposit is cut by coarser material, composed exclusively of poorly sorted gravel. This sandy unit contains a highly variable concentration of charcoal and micro-charcoal that might reflect episodic continental inputs. A silty peat deposit containing many plants remains (plant fibres and charcoal) is encountered at an elevation ranged from ca. -0.3 to +0.8 m asl, according to the trenches studied (Fig. 7). Along the QT3, the peat is overlaid with ca. 0.5 m thick, coarse sand deposit, with a high proportion of shell and plant debris. The contact between this coarse deposit and the underlying peat layer is very sharp, which indicates erosion of the surface. The thickness of this unit decreases seaward from 0.5 m to 0.2 m, and suggests paleo-relief parameters, potentially related to the ancient position of the Wadi Munayzif mouth, or to its paleo-floodplain. From ca. +1 to +1.4 m asl, the sediment sequence is composed of a yellowish, sandy-silt material with fine and regular bedding, organized in small lamina a few centimetres long. It is associated with a progressive clogging of the plain by low-flow dynamics or runoff (alluvium and colluvium). The upper part of the sequence is an aeolian sand with cross stratification (reworked).

398

#### 4.2.2. Dune fields area

400

Our investigations on the dune fields area showed the base of the sediment sequence is composed of a ca. 2 m mean thick coarse shelly sand (Fig. 7). A thin peat deposit ca. 0.3 m thick is observed in core QU7. From ca. -1.2 to + 2.6 m asl, a sandy-silty sediment with fluvial

402

facies is observed. Two thin greenish silty-clay layers are interbedded into this deposit,  
404 indicating readjustments to the edges of coastal environments. As in the Wadi Dayqah delta  
area, the upper part of the sequence is composed of aeolian sands with a 3 m thickness on core  
406 S1 (Fig. 7). The base of this unit exhibits few bedded laminas, which we interpret as the runoff  
reworking of aeolian sands.

408

#### 4.2.3. The sebkha area

410

In the sebkha of Quriyat, the base of the sediment sequence is composed of shelly, fine  
412 to medium sand. The thickness of the deposit varies from ca. 0.4 to 2 m (Fig. 7). The cores  
located in the outer part of the sebkha (QU3 and QU6) show the thickest sandy deposits, thus  
414 indicating the predominance of marine sedimentation close to the sea. From ca. -0.80 to +0.40  
m asl, we observed a peat deposit comprising numerous, vegetal remains (fibre, charcoal), and  
416 shells of *Terebralia palustris*, with a thickness varying from 0.3 to 0.9 m (Fig. 7). The peat  
layer is overlaid by relatively thin layers of marine sediments, varying from shelly sand (QU3)  
418 to fine gleyed sand (QU6). The cores located in the innermost part of the sebkha (QU2 and  
QU5) have a very thin sandy deposit, with low proportion of shell fragments, while the  
420 underlying peat layer is well-developed, and contains numerous charcoal deposits (Fig. 7). The  
upper part of the sediment sequence exhibited a sandy silt to silty sand deposits. Evaporite  
422 incrustations are observed in QU3 at an elevation of +1.42 m asl, and indicate a depositional  
environment corresponding to that of the sebkha.

424

#### 4.3. The QT3 sequence

426

The sediment sequence studied along the QT3 trench (Fig. 5 and Fig. 8) is composed of  
428 a series of 12 different sediment facies (SF), distributed from -2.8 to +1.53 m asl (Fig. 8).

At the base of the sequence, a 2.6 m thick series of sandy to silty deposits clustering the  
430 SF1 to SF8 (Fig. 8), matched the SU1 observed in the stratigraphy of the Quriyat coastal plain  
(Fig. 7). SF1 to SF3 are characterized by silty material, with a median grain size below 50  $\mu\text{m}$ .  
432 A sharp contact, corresponding to a level of pebbles with an average diameter of about 5 cm, is  
observed between SF1 and SF2. The median grain size increases in the upper SF4 and SF5 and  
434 is associated to coarse sand deposits. The proportion of sediments ranged between 500 and 2000  
 $\mu\text{m}$  reaches 60% in the SF5. The foraminifera assemblages are clearly dominated by marine  
436 and hyperhaline species (Fig. 8), indicating an open lagoon context (Fig. 6). The SF5 to SF7  
corresponded to an alternation of fine sand (50 to 200  $\mu\text{m}$ ) to medium sand (200 to 500  $\mu\text{m}$ )  
438 deposits. The micro-faunal content shows a larger part of brackish water species, such as  
*Elphidium gerthi*. The SF8 displays a 1.15 m thick, relatively homogeneous silty and fine sandy  
440 sediment, characteristic of a low hydrodynamic environment. The base is dated from 7183-  
7416 cal. BP (Table 1).

442 The SF9 and SF10 identified in the QT3 trench are associated to the SU3, and  
correspond to peat levels. The SF9 consisted of an organic-rich, fine and medium sand  
444 containing numerous vegetable fibers, as shown by the large size of granulometric fractions,  
before their treatment with hydrogen peroxide. The SF10 consisted of a silty peat of 0.4 m thick,  
446 whose base is dated to 6501–6712 cal. BP (Table 1). Foraminifera were absent from this unit,  
as from the other peat units studied in the coastal plain.

448 The SF11 and SF12 correspond to a shell deposit embedded into a silty to sandy matrix.  
These facies could be associated to the SU4 (Fig. 8). The coarse fraction correspond to shell  
450 debris exceeding 50% of the total weight of samples in SF11. The coarse fraction decreased  
both in size and proportion in the SF12, reaching only 20% of the total sediment. When only

452 considering the fine fraction (matrix), we noted an increase of the median grain size, from the  
base to the top of the SF11, then a decrease of the median grain size into the SF12. The  
454 treatments with hydrogen peroxide and hydrochloric acid, highlighted the high organic matter  
content of SF11. This unit had a large amount of plant debris at its base, some of which are  
456 pluri-centimetric. SF12 is very rich in carbonates due to the high density of shell fragments.  
Very few specimens of foraminifera were found, except for two *Miliolids sp.* in SF11, and three  
458 *Amphistegina sp.* in SF12 (Fig. 8). Analysis of shell remains in SF11 showed assemblages  
dominated by *Ostrea* and *Anadara*, two intertidal species (although *Anadara* ranges from  
460 mangrove mud to subtidal sands). The presence of *Nerita textilis*, normally found in rocky  
coasts, indicated a possible mixing of the shells due to the relative distance of the nearest rocky  
462 coasts (6 km to the south). Finally, the rather blunt and friable taphonomy of shells indicated a  
possible reworking/rolling by coastal currents and waves.

464 The upper part of the QT3 sequence (SF13 to SF15) correspond to the US6, recognized  
in the Quriyat coastal plain (Fig. 7). The base is dated from 5992-6183 cal. BP (Table 1). These  
466 facies are characterized by a silty sediment with no foraminifera and molluscs, except in the  
upper part where the assemblages are only composed of the *Ammonia sp.* (*Ammonia tepida* and  
468 *Ammonia inflata*). These particularly tolerant species probably point to an increasingly  
restrictive environment. Finally, SF15 consist of a bedded silt deposit (Fig. 8).

470

#### 4.4. Core QU4

472

The core QU4 (Fig. 4) is composed of a succession of 10 sediment facies (noted SF1 to  
474 SF10, Fig. 9), associated to the main stratigraphic units identified within the coastal plain of  
Quyirat (Fig. 7). From -1.46 to -0.8 m asl., the base of the core is composed of a bioclastic,  
476 grey coarse sand (SF1), corresponding to the SU1 identified in the stratigraphy of the coastal

plain. The malacological spectrum includes both subtidal species (*Rhinoclavis fasciata* and  
478 *Nassarius castus*) and intertidal species associated with various habitats (Fig. 9). *Umbonium*  
*vestiarum* is mainly observed on the sandy seafloors, while *Trochoidea* and *Rhinoclavis kochi*,  
480 preferred the rocky seafloors (Fig. 6). The studied shells are highly fragmented with a strong  
angular shape of the fragments. The foraminifera assemblage is dominated by the *Miliolids*  
482 species (named "assemblage *Miliolids sp.*"). *Miliolids* preferentially settle in open lagoon  
environments with very limited freshwater inputs. They were found in high concentrations in  
484 the distal and central parts of the Sur lagoon (Pilarczyk *et al.*, 2011). They enjoy hypersaline  
environments and sandy substrate (Leckie, Olson, 2003), and are absent from brackish  
486 environments. Although *Miliolids* characterize calm environments, they can develop in high-  
energy environments, near coral reefs (Saraswati, 2002). *Miliolids* assemblage are associated  
488 with *Ammonia tepida* (Cushman, 1936; Debenay, 1998) and *Ammonia parkinsoniana*  
(D'Orbigny, 1839). These two species develop in brackish to hypersaline environments. As they  
490 have strong ecological tolerance, they cannot be considered as precise bio-indicators.

From -0.8 to -0.45 m asl, the series of sediment facies (SF2 to SF4, Fig. 9) is  
492 characterized by a grey coarse sand, with highly fractured shell debris. These facies correspond  
to the SU2. Foraminifera assemblages are dominated by *Ammonia sp.* and *Elphidium sp.*, with  
494 a predominance of *E. advenum* (Cushman, 1936), *A. parkinsoniana* and *A. tepida* (Fig. 9). This  
assemblage was named "*Ammonia sp. / Elphidium sp.* assemblage". A high proportion of *E.*  
496 *advenum* is observed at the base of the SF9, and associated with coarse and fractured shells,  
between -0.80 m and -0.75 m asl *E. advenum* was replaced by *E. gerthi* (Van Voorthuysen,  
498 1957) in the upper part of the SF9 (Fig. 9). *Miliolids* were totally absent from this assemblage,  
which may reflect an environment influenced by episodic freshwater inputs, or by the gradual  
500 closure of the lagoon to the sea. The top of the SF2 is dated from 3981-4150 cal. BP (Table 1),

a time during which vegetable fibres were abundant, and associated with the gradual decrease  
502 of the median grain size (Fig. 9).

From -0.46 to +0.34 m asl, a clayey to silty, very dark coloured peat, containing a high  
504 concentration of vegetable fibres and coals was observed. This sediment facies was associated  
to the SU3 (Fig. 9). The malacological analysis of the few shells sporadically present in this  
506 unit, indicates the presence of *Terebralia palustris*, which is specific to mangroves.  
Foraminifera were absent from this deposit, thus indicating a freshwater environment.

508 From +0.34 m to +0.43 m asl, a fine gleyed sand (Munsell code: 7.5 YR 6/8, Gley 1 6/1  
Greenish grey) corresponded to a hydromorphic sediment, associated to the SU5. This facies  
510 was thin in core QU4, but reached about 1 m thick in other cores, such as QU2 (Fig. 7). The  
presence of red spots in the sediment indicates iron precipitation, and regular exposition of the  
512 depositional surface to the oxidation processes by the air, probably during periods of  
desiccation. The foraminifera assemblage (named "*Ammonia tepida*" assemblage) were largely  
514 dominated by *A. tepida* (Fig. 9). This euryhaline species tolerates high variations of salinity and  
temperature, as well as reduced oxygen conditions (Debenay, 1990). The final part of this unit  
516 is dated from 2510–2757 cal. BP (Table 1).

The upper part of the core QU4 is a 1.5 m thick bedded silt and fine sand deposit (SF7  
518 to SF10), without any marine faunal and shells (Fig. 9). This sediment unit corresponds to the  
SU6, deposited by low-energy sheet flows. The top of this fluvial sequence is a homogeneous  
520 silt layer, leached from its clays, and slightly crystallized, thus indicating a sebkha environment.

#### 522 **4.5. Supplementary sedimentological analyses and datings**

524 To complete the interpretation of the sediment successions studied in the coastal plain  
of Quriyat, additional information was obtained from the other cores performed in the dune

526 field area. A first sample collected at the base of the QU8 core (between -1.91 and -1.96 m  
asl) presented a "*Miliolids sp.* assemblage", which reflects an open and dynamic lagoon  
528 environment. A second sample collected in the lower part of the QU7 core (between -0.50 and  
-0.55 m asl) also showed a significant dominance of *Miliolids sp.* The QU7 core was also  
530 sampled at the elevation of -0.40 m asl for radiocarbon dating. The collected material dated  
from 3984–4223 cal. BP, for the transition between shelly sand deposit (SU1) and peat layer  
532 (SU3). This result is consistent with the other age-dating obtained from the Holocene deposits  
of the Quriyat coastal plain.

534

## 5. Discussion

536

### 5.1 Reconstitution of the Quriyat coastal plain

538

#### 5.1.1 Before 7416–7183 cal. BP: an environment with marine influence, typical of an open 540 lagoon

The chronostratigraphic starting point to our reconstruction is provided by the sandy  
542 lagoon units of the QT3 base, after 7416–7183 cal. BP. The sedimentological and micro-faunal  
characteristics of these units refer to a lagoon environment with marine influence, while the  
544 grain-size variability, alternating between coarse and fine sands, refers to flow dynamics,  
potentially linked to tides, currents or surges. Those units are interpreted as deposits from an  
546 open lagoon, bounded by barrier islands or by a sand spit (Fig. 10). The QT3 basal deposits  
would be related to the inner part of the sand spit, or to a tidal inlet. Its position, 2.5 km from  
548 the present-day coastline, indicates a significant, horizontal retreat from the shoreline to the  
land, after deposition. Our reconstruction of the relative sea-level, based on "sea-level index



550 points" (Hijma *et al.*, 2015) (Fig. 11), indicates that the current sea-level (+/- 1.5 m) in Quriyat  
is similar to the sea-level from 7416–7183 cal. BP.

552

### 554 **5.1.2. Between 7416-7183 cal. BP and 6712-6501 cal. BP: the beginning of progradation and the development of mangroves**

Sediments and micro-fauna from SF8 to SF10 (QT3) refer to a calm lagoon  
556 environment, starting from 7416-7183 cal. BP, and then developing into mangroves around  
6712-6501 cal. BP. This evolution certainly coincides with the formation of a stabilized sand  
558 bar, leading to the progressive confinement of the environment (Fig. 10). The presence of  
mangroves may have favoured the deposition of fine sediments (as silts were mainly observed  
560 in this unit). Radiocarbon dates obtained by Berger *et al.* (2013) for the 5a section in Alashkara  
indicate a maximum of mangrove development in Ja'alan between  $6410 \pm 40$  BP and  $5535 \pm$   
562  $40$  BP. By using the same calibration procedure described in section 3.6 for these two  
radiocarbon ages, we replace this period from ca. 7350 cal. BP to 6340 cal. BP, indicating a  
564 concomitant mangrove forest evolution for the two coastal sites of Ja'alan and Quyirat.

The influence of a regional forcing, such as wetter climatic conditions (an influence  
566 from the Holocene humid period) and a stability of the relative sea-level, is suggested by the  
data obtained in Quriyat and Ja'alan. Indeed, the establishment, or even the progradation of low  
568 accumulation patterns, is favoured by stable sea-levels, while mangrove expansion is  
incompatible with transgressive episodes (Ellison and Stoddart, 1991). At the same time,  
570 intense rainfall can lead to fluvial activity, providing sediment inputs for sand bar fattening, and  
fresh water for mangrove feeding. In Lézine *et al.* (2017), pollen analyses by Kwar al Jaramah  
572 revealed the gradual development of drier climatic conditions between ca. 5000 and 4500 cal.  
BP, in correlation with the southern shift of the monsoon boundary (Fig. 1 and Fig. 11). This  
574 resulted in the decline of the *Rhizophora* taxon, ranging from tropical to humid subtropical

climates, to the benefit of *Avicennia* or *Artemisia*. In Quriyat, fluvial records tend to confirm  
576 that rainfall was maintained up to ca. 4500 cal. BP. Indeed, alluvial accumulation was still  
important during the edification of the T4 alluvial level. Near Wadi Miglas and Wadi Qahmah  
578 (Fig. 3), the T4 alluvial level has an advanced position compared to that of the current shoreline.  
It can attest the T4 alluvial accumulation is at least contemporaneous to the position of the  
580 shoreline.

Finally, the establishment of stabilized sand bars, and the development of mangroves  
582 are consistent with a Neolithic occupation, dated from the end of the 5th millennium / beginning  
of the 4th millennium, as well as with the construction of Khor Milk I and II shell middens  
584 (Phillips and Wilkinson, 1979) along the current Wadi Munayzif. We can consider that men  
settled on the most stable part of the sand bar, and went fishing in the open sea. The high density  
586 of micro-charcoal and macro-charcoal in the SF8 of QT3, can be considered an indirect,  
anthropogenic signal, linked with the exploitation of the environment. Indeed, in Suwayh 1 and  
588 Ra's al Hamra 5 and 6, mangrove exploitation by Neolithic populations is visible from the 5th  
millennium until ca. 3500 BC (about 6500 and 5450 cal. BP) (Tengberg, 2005).

590

### **5.1.3. Between 6712-6501 cal. BP and 6183-5992 cal. BP: an overwash event**

592 SF11 and 12 are interpreted as an overwash deposit. Several criteria were used to try to  
discriminate between the meteo-oceanic and tsunamic nature of this hazard. First, general  
594 sedimentological and physical criteria were analysed: as tsunamis bring along a lot of  
suspended matter, they tend to deposit lateral, extensive sandy units, including intra-clasts and  
596 "muddy" lamina. According to Morton *et al.* (2007) and Donato *et al.* (2009), the thickness of  
a tsunami deposit is rather homogeneous (< 0.25 m), and has a decreasing thickness towards  
598 the continent as well as a normal or inverse granulometric classification. On the other hand, due  
to the transport of numerous materials through the hauling process, the storm deposits are

600 presented in series, organized into several units with normal or inverse classification. The  
thickness of the deposit, generally exceeding 0.3 m, reaches its maximum near the shore, and  
602 decreases sharply as it moves inland. Storm deposits are found within 300 m of the shoreline,  
and contain little or no muddy intercalations (Morton *et al.*, 2007; Donato *et al.*, 2009).

604 Secondly, we compared our data with the sedimentological, granulometric, malacological,  
and micro-faunal characteristics of the 1945 tsunami deposits in the Sur lagoon,  
606 100 km south of Quriyat. These deposits have an average thickness of 0.4 m, with a rather  
coarse grain size, averaging between 200  $\mu\text{m}$  and 500  $\mu\text{m}$ , and mainly containing coarse shell  
608 debris with significant fracturing. A few articulated shells were present in the debris, but were  
not observed in living position (Donato *et al.*, 2008). All shell debris are composed of species  
610 belonging to the upper intertidal, or subtidal zones (Donato *et al.*, 2008; Donato *et al.*, 2009).  
The micro-fauna is present in sufficient quantity in the event units to be used as a parameter.  
612 The foraminiferous taxa, most useful to identify overwash events, are *Amphistegina sp.*,  
*Ammonia inflata*, *Elphidium advenum*, and planktonic foraminifera, as they occur in marine  
614 and subtidal environments (Pilarczyk *et al.*, 2011).

Based on the general physical, and sedimentological discrimination criteria, and on the  
616 grain size characteristics of the Sur deposit, the characteristic of the unit studied in QT1, QT2  
and QT3, is closer to a tsunami than to storm deposits. This is due to: 1) its thickness (<0.7 m  
618 in places); 2) its granulo-grading decreasing from SF11 to SF12; 3) sandy matrix sealing highly  
fractured shell debris; 4) the high number of clay inclusions; 5) mat of plant remains at the base  
620 of SF11; 6) the rather intertidal origin of the shells composing the debris (with a high proportion  
of *Ostrea sp.* and *Anadara sp.*). On the other hand, the foraminifera signal is very weak, or even  
622 contradictory. They are practically absent in SF11 and SF12, except for three individuals  
belonging to the taxa *Amphistegina sp.* and *Milioida sp.* Such an absence of foraminifera tends  
624 to suggest the sudden remobilization of sandy-shelly material located outside the foreshore,

such as the exposed part of a sand bar that apparently was brutally displaced. The event is dated  
626 between 6712–6501 cal. BP and 6183–5992 cal. BP, two millennia before the submergence  
deposit, identified by Hoffmann *et al.* (2015) on the archaeological site HD-6 at Ras al Hadd,  
628 and dated 4450 cal. BP. There are no other regional occurrences.

#### 630 **5.1.4. Before 4223-3984 cal. BP and 4150-3981 cal. BP: a lagoon environment occupying most of the Quriyat plain**

632 The analysis of sediment cores carried out in the centre and the northern part of the  
Quriyat coastal plain attests to the presence of lagoon environments, up to 4223-3984 cal. BP  
634 (see cores QU4 and QU7 on Fig. 10). Malacological and micro-faunal assemblages identified  
in the lower part of the core QU4 indicate a gradual change from an open lagoon environment  
636 to more sheltered conditions. Angular shape shells debris observed from SF1 to SF2 (Fig. 9)  
are interpreted as beach material transported through a tidal inlet and deposited to the inner part  
638 of the lagoon. Shells debris are associated with foraminifera assemblages dominated by  
*Miliolids*. From SF3 to SF4, the transition to a bio-facies dominated by *Ammonia/Elphidium*  
640 assemblages reflects a decrease in the salinity rate related to a closure of tidal inlets or to an  
increase in freshwater inputs from Wadi Qahmah (possibly due to an avulsion).

642

#### 644 **5.1.5. Between 4150–3981 and 2757–2510 cal. BP: rapid clogging of the lagoon, as mangroves remain in the northern part of the plain**

In the upper part of the sediment cores studied, shell sand units, characteristic of lagoon  
646 environments, are clearly replaced by continental sediments. Such a change in the sedimentary  
facies attests to the extended lagoon being closed. This transition was dated in QU4 and QU7,  
648 and was carried out over a very short period, possibly in the order of a decade, i.e. between  
4223–3984 cal. BP and 4150–3981 cal. BP. The infilling of the coastal plain by alluvial

650 sediment extend over long distances, i.e. 3.8 km between QU7 and QU4. This very rapid and  
spatially extensive clogging should be considered as the consequence of a major alluvial crisis,  
652 or as a phase of aeolian accumulation. It may be related to the sudden start of arid conditions,  
identified in the pollen records of Kwar-al-Jaramah at ca. 4500 cal. BP (Lézine *et al.*, 2017). It  
654 might also be linked to macro-regional fluctuation, such as the "4200 BP" arid event. The latter  
caused intense detritism in the Hadramawt rivers (Yemen) (Berger *et al.*, 2012), favoured the  
656 reactivation of dune accumulations in Liwa (UAE) (Stokes and Bray, 2005), as well as the  
sealing of the Ja'alan sebkhah (Oman) (Berger *et al.*, 2013). This arid event caused a significant  
658 adjustment in the Quriyat lagoon, which is clearly retreating to the northwest. The mangrove  
swamps also followed this northward migration. The mangrove peat is stable at the QU4 level,  
660 from 4150–3981 cal. BP to 2757–2510 cal. BP.

#### 662 **5.1.6. From 2757-2510 cal. BP: the development of coastal sebkhah and dune fields**

The *Ammonia tepida* assemblage, identified in the upper part of the QU4 peat unit,  
664 reflects significant reducing conditions, and an asphyxiated environment. The soils associated  
with this monospecific assemblage are oxidized hydromorphic soils (redox). They are  
666 characteristic of anaerobic environments with a limited oxygen supply, one that is not  
conductive to the development of vegetation.

668 From 2757–2510 cal. BP, hydromorphic soils were sealed under 1.5 m thick of fluvial silts.  
The bedded silts ended with increasingly dense gypsum crusts, indicating a sebkhah  
670 environment. This alluvial clogging was generated by weakly dynamic flows, either related to  
settling deposits on the distal part of the floodplain, or to remobilizing aeolian fine material. It  
672 is visible in every core carried out in the Quriyat plain, and therefore pertains to the entire  
hydrographic network. Alluvial infilling may have been favoured by an erosive crisis after  
674 2757–2510 cal. BP. Such a hypothesis is supported by a late alluvial accumulation identified at

Hadramawt between ca. 2700 and 2000 BP (Berger *et al.*, 2012), and by a moisture peak  
676 identified in Filim's pollen records (Lézine *et al.*, 2017). An increase in rainfall is also supported  
from other watersheds related to the Hajar mountains, such as in Masafi (United Arab  
678 Emirates), where a runoff-water channelling and a high aquifer were identified between ca.  
3000 and 2500 cal. BP (Purdue *et al.*, 2019).

680 No age-dating was carried out for the most recent units, made of aeolian sand or gypsum-rich  
silts. The dunes started to develop after alluvial landings, at least after 2757–2510 cal. BP. The  
682 khabras, mainly composed of fine silts, certainly have an aeolian origin, and would have been  
captured and forced to deposit, by plants or natural obstacles (such as palm trees from an oasis  
684 or the reliefs surrounding the plain).

## 686 **5.2. The important palaeogeographic evolution of Quriyat: a significant taphonomic bias for identifying archaeological sites in the low-lying part of the coastal plain**

688

### **5.2.1. Relative sea-level stability at Quriyat**

690 The shoreline changes of Quriyat indicates a significant progradation of the coastal  
sedimentary prism over the last ca. 7000 years cal. BP. The calculation of "sea-level index  
692 points" (Hijma *et al.*, 2015) indicates this evolution was favoured by a relative sea-level stability  
since 7416-7183 cal. BP. These results significantly differ from other relative sea-levels  
694 obtained in the Ja'alan. They are comprised between +3 and +5 m compared to the present  
values (Berger *et al.*, 2013), around 7500 cal. BP in Ja'alan, and As Suwayh (Berger *et al.*,  
696 2005) (Fig. 11). Such differences can be explained by the uplift of the coastal portion of the  
Ja'alan coast. The part of the coastline south of Quriyat shows the two active, reverse faults of  
698 Qalhat and Ja'alan, whose vertical activity is one of the most important in the region (Moraetis  
*et al.*, 2018). Indeed, the rate of uplift for this coastline stretch during the Middle Holocene was

700 estimated to average 1 mm/year (Moraetis *et al.*, 2018). This rate corresponds to the Ja'alan  
sea-level index points identified at +5 m, and dated between ca. 7450 and ca. 3950 cal. BP by  
702 Berger *et al.* (2013), and Berger *et al.* (2005).

Therefore, the Omani coast between Quriyat and Ja'alan is divided into several tectonic  
704 compartments, either characterized by uplift or subsidence, and exhibiting various landscapes  
and landforms. For instance, all the areas studied by Moraetis *et al.* (2018), and Falkenroth *et*  
706 *al.* (2019), show ablation and landform deposits related to uplift (marine terraces, notches), but  
whose development or altitudes refer to variable uplift rates, depending on the area. In the  
708 Quriyat area, neither quaternary marine terraces, nor notches were identified, due to the  
subsidence of the Quriyat coastal plain.

710 The role played by neo-tectonics in the apparent stability of the relative sea-level, could  
not be quantified. It seems the Quriyat compartment has stabilized at +/- 1.5 m since 7416–7183  
712 cal. BP. The lack of visible archaeological sites in the Quriyat plain may be explained by the  
combination of a significant Holocene silting up, and of a subsidence favouring the burial of  
714 fossil forms.

### 716 **5.2.2. The silting up of the plain**

Despite the subsidence, Quriyat is one of the few prograding coasts in Oman. Since the  
718 Middle Holocene, between 7416–7183 and 2757–2510 cal. BP, the lagoon has been silting up  
significantly, due to important aeolian and fluvial sedimentary inputs, which have clogged  
720 extensive lagoon environments, and transformed some of them into sebkhas.

The main part of the fluvial material comes from Wadi Dayqah. The well-developed  
722 lobe of its delta shows an extra sedimentary budget, sufficiently large for it to be at the origin  
of deltaic prograding forms, despite the mesotidal context (3 m of average tidal range at  
724 Quriyat). Once they reach the tidal outlet, sediments from Wadi Dayqah are redistributed

laterally by a northwest-trending coastal longshore drift. Coastal currents play a decisive role  
726 in the fattening of sand bars, which define the lagoon's water body and its filling. Wadi  
Dayqah's influence is visible through the asymmetric progradation of the plain, and through  
728 the clogging progress of the lagoon environments. Also, the latter persist longer in the northern  
part of the plain than in its southern part, directly exposed to the Wadi Dayqyah delta  
730 sedimentary input. Therefore, the closure occurs from southwest to northwest, and favours the  
moving of intertidal ecosystems, such as mangroves, towards the north.

732 Fluvial accumulation is subject to high temporal variability, and is particularly  
important at the end of arid episodes occurring at a regional scale. The rapid closure of lagoon  
734 environments over several kilometres, between 4223–3984 cal. BP and 4150–3981 cal. BP, i.e.  
a few decades, was probably caused by a major erosive crisis, possibly following the regional  
736 aridity peak event of 4200 BP, mainly registered from the Mediterranean area to Asia (Giesche  
*et al.*, 2018; Kaniewski *et al.*, 2018). The fluvial sequence of QU4 (as well as all QU cores)  
738 indicates fluvial infilling is made of silty to very fine sands. It suggests our samples were  
realized in the distal parts of wadis, and can be reached only by decantation deposits. This  
740 alluvial infilling is very different from the bedload deposits we can observed in the braid-belt.  
Associated with alluvial clogging, the rapid drying of the lagoon is also caused by a high  
742 evaporation rate, and higher aeolian sedimentary inputs.

The study of the river palaeoflora highlighted a differential preservation of alluvial  
744 terraces, both in the northern and southern part of the plain. This difference can either be  
explained by a deeper incision of Wadi Miglas, related to hydrodynamic or neotectonic causes  
746 (such as a greater subsidence north of the plain), or/and by a higher erosive capacity of Wadi  
Dayqah, at the time the T4 alluvial level was formed. Indeed, the Wadi Dayqah delta seemed  
748 to be subject to more violent floods than those of Wadi Miglas. It could lead to significant re-



750 mobilisation of alluvial material belonging to the T1, T2 or T3 levels, and to its transport into  
the sea.

### 752 **5.2.3: The interactions between the coastal environment and the archaeological presence at Quriyat**

754 Between 7416-7183 cal. BP and 6712-6501 cal. BP, Wadi Dayqah presented an open  
lagoon, and a well-developed mangrove. The closeness to these attractive environments  
756 favoured the settlement of Neolithic populations, and the building of the Khor Milk I and II  
shell middens. The presence of *Terebralia palustris* in the shell midden deposits attests the  
758 populations used to live close to the mangrove. The discovery of numerous hooks and stone  
fishing sinkers on these shell midden (Uerpmann, 1992) testify that people lived close to the  
760 open sea environment, possibly on a sand barrier, and exploited seafood resources. Neolithic  
occupations relied on similar subsistence strategies used by other populations on the Omani  
762 coast. Unlike in other areas (Shiya and Ja'alan), evidence of Bronze Age occupation is very  
scarce at Quriyat, as it relies on a few graves, despite the presence of mangrove environment  
764 until ca. 4000 cal. BP. The highly variable speed and rate of the clogging of the lagoon, from  
ca. 6000 to ca. 4000 cal. BP, might have impacted the preservation of Neolithic and Bronze  
766 Age landscapes and archaeological sites. In Quriyat, it is highly possible that the low and  
unstable parts of the prehistoric and protohistoric plain, have either disappeared under more  
768 recent sedimentary layers (such as fluvial or aeolian silt/sand), or were dismantled. Such  
variations make an important taphonomic bias in the preservation, and visibility of prehistoric  
770 and protohistoric sites in Quriyat. They help us to explain the rarity of the sites discovered in  
this sector, despite its strong ecological attractiveness, consisting of mangroves until the end of  
772 the middle Bronze Age. Indirect signs of anthropization, visible in the numerous charcoals  
trapped in the QU cores, and also visible in the trenches, suggest the plain was not deprived of

774 archaeological sites. Even though no Late Bronze Age site was discovered in Quriyat, this  
period (3450–3250 cal. BP) regionally refers to a “dark” period, as it lacks archaeological  
776 findings and data. This lack of information may be interpreted as a demographic fall, or as an  
abandoning of site locations and permanent buildings, and linked to the aridification of climate.  
778 Again, no site from the Iron Age (between 3250–2250 cal. BP) was discovered in Quriyat,  
despite significant presence on the neighbouring coasts (Besenval *et al.*, 2014; Loreto, 2015).  
780 It is possible the coastal plain was no longer attractive, even with a small increase in rainfall;  
alternatively, the aeolian sedimentary infilling, occurring during this period, may have covered  
782 the Iron Age archaeological sites.

The ephemeral nature of old settlements raises questions about the sustainability of  
784 current occupations, particularly those produced out of the urban sprawl of the last ten years.  
Residential neighbourhoods mainly develop on the T4 terraces or near the wadis’ floodplains,  
786 where exposure to the flooding hazard is the highest. This hazard was particularly important  
during tropical cyclones, and caused many damages during the passage of cyclones Gonu and  
788 Phet in 2007 and 2010, respectively. The increase in emerging cyclones in the northern Indian  
Ocean, due to global warming and to rising surface water temperatures (Krishna, 2009),  
790 suggests an intensification of morphogenic events in the coastal plain of Quriyat. Thus, our  
long-term study tends to highlight the current exposure of the Quriyat plain to wadi floods and  
792 coastal risks, particularly threatening the newly urbanized areas located on the T4 terraces.

## 794 **6. Conclusion**

For the first time, a multidisciplinary study, based on the understanding of current and  
796 past geomorphological dynamics, as well as on paleoenvironmental and sedimentological  
analyses, has allowed us to suggest a scenario of the evolution of the Quriyat plain, from the  
798 Middle Holocene to the Recent Holocene. The paleogeographical reconstructions have shown

significant horizontal shifts of the coastline, and the importance of river and wind dynamics in  
800 the rapid sealing of the Quriyat coastal lagoon. The sedimentary filling of the lagoon shows  
irregular rates of sedimentation: an overwash event, probably tsunamigenic, filled ca. 0.7 m  
802 thick of shell debris; the peak aridity at 4200 BP dried up 3 km of lagoon in a few decades;  
from 2757–2510 cal. BP up to the present-day, 1.50 m thick of bedded silt has been deposited  
804 in the Quriyat sebkha, thus pointing to a slow and gradual clogging of a few millimetres per  
year, while 15 m high dunes are present one kilometre further away. In Quriyat, such dynamics  
806 have important taphonomic implications, and can partially explain the rarity of visible  
archaeological remains, despite the strong attractiveness of its ancient coastal environments.

808

### **Acknowledgements**

810 This study is supported by the MEDEE programme led by Éric Fouache, and funded by the  
Ministry of Foreign Affairs. We would like to thank the Sorbonne Abu Dhabi Research Fund  
812 attributed to Kosmas Pavlopoulos, for its participation in the funding of the dates. We would  
also like to thank the Ministry of Culture and Heritage of the Sultanate of Oman, for its  
814 administrative and technical support. Our thoughts go out to Roland Besenval, who initiated  
the resumption of surveys in 2013, in the Quriyat area. We would like to thank Daniel Étienne  
816 of EVEHA, and Daniel Moraetis of Sultan Qaboos University, for their assistance in  
topographic operations, as well as the entire French archaeological mission to Qalhat, for their  
818 logistical assistance on the field. We also thank Mohamed Abdullah Ahmed Al Dhari, Saleh Al  
Muharrami, and Hugo Naccaro, for their help during the drilling of cores, and Mohammed al  
820 Busseidi from Quriyat, for his hospitality and support. Finally, we are very grateful to Gösta  
Hoffmann for its constructive comments.

822

824 **References**

- 826 Almathen, F., Charruau, P., Mohandesan, E., Mwacharo, J.M., Orozco-terWengel, P., Pitt, D.,  
Abdussamad, M.A., Uerpmann, M., Uerpmann, H.P., De Cupere, B., Magee, P., Alnageeb, M.A.,  
828 Salim, A., Raziq, A., Dessie, T., Abdelhadi, M., Banabazi, H., Al-Eknaah, M., Walzer, C., Faye, B.,  
Hoffreiter, M., Peters, J., Hanotte, O., Burger, P.A., 2016. Ancient and Modern DNA reveal  
830 dynamics of domestication and cross-continental dispersal of the dromedary. PNAS. 113 (24),  
6707–6712.
- 832
- Azzara, V., 2013. Architecture and buildings techniques at the Early Bronze Age site of HD-6, Ras al-  
834 Hadd, Sultanate of Oman. Proceedings of the Seminar for Arabian studies. 43, 11–26.
- 836 Azaz, L. K., 2010. Using Remote Sensing and GIS for Damage Assessment after Flooding, the Case of  
Muscat, Oman after Gonu Tropical Cyclone 2007: Urban Planning Perspective. REAL CORP 2010  
838 Proceedings/Tagungsband. (18-20 May 2010), Vienna
- 840 Bailey, G.N., Devès, M.H., Inglis, R.H., Meredith-Williams, M.G., Momber, G., Sakellariou, D.,  
Sinclair, A.G.M., Rousakis, G., Al-Ghamdi, S. Alsharekh, A.M., 2015. Blue arabia: Palaeolithic  
842 and underwater survey in SW Saudi Arabia and the role of coast in Pleistocene dispersals.  
Quaternary International. 382, 42–57.
- 844
- Besenval, R., Beuzen-Waller, T., Desruelles, S., Fouache, E., 2013. Report of the French-Italian  
846 geoarchaeological program in the Sur-Quriyat area, Ministry of Heritage and Culture of the Sultanate  
of Oman, unpublished
- 848
- Berger, J.-F., Cleuziou, S., Davtian, G., Cattani, M., Cavulli, F., Charpentier, V., Cremaschi, M., Giraud,  
850 J., Marquis, P., Martin, C., Mery, S., Plaziat, J.-C., Saliège, J.-F., 2005. Évolution

- paléogéographique du Ja'alan (Oman) à l'Holocène moyen : impact sur l'évolution des  
852 paléomilieux littoraux et les stratégies d'adaptation des sociétés humaines. *Paléorient*. 31, 46–63.
- 854 Berger, J.-F., Bravard, J.-P., Purdue, L., Benoist, A., Mouton, M., Braemer, F., 2012. Rivers of the  
Hadramawt Watershed (Yemen) during the Holocene: Clues of Late Functioning. *Quaternary*  
856 *International*. 266, 142–61.
- 858 Berger, J.-F., Charpentier, V., Crassard, R., Martin, C., Davtian, G., Lopez-Saez, J.A., 2013. The  
dynamics of mangroves ecosystems, changes in sea-level and the strategies of Neolithic settlements  
860 along the coast of Oman (6000-3000 cal. B.C.). *Journal of Archaeological Science*. 40, 3087–3104.
- 862 Beuzen-Waller, T., Giraud, J., Gernez, G., Courault, R., Kondo, Y., Thornton, C., Cable, C., Fouache,  
E., 2018. L'émergence des territoires proto-oasiens dans les piémonts du Jebel Hajar. *Acte des*  
864 *XXXVIII<sup>e</sup> rencontres internationales d'archéologie et d'histoire d'Antibes*. 179–205.
- 866 Biagi, P., 1994. A radiocarbon chronology for the aceramic shell-middens of coastal Oman. *Arabian*  
*Archaeology and Epigraphy*. 5, 17–31.
- 868
- Charpentier, V., Angelucci, D., Méry, S., Saliège, J. -F., 2000. Autour de la mangrove morte de Suwayh,  
870 l'habitat VI-V millénaire de Suwayh SWY-11, Sultanat d'Oman. *Proceedings of the Seminar for*  
*Arabian Studies*. 30, 69-85.
- 872
- Charbonnier, J., 2015. Groundwater management in Southeast Arabia from the Bronze Age to the Iron  
874 Age: a critical reassessment. *Water History*. 7 (1), 39–71.
- 876 Debenay, J.-P., Bénéteau, E., Zhang, J., Stouff, V., Geslin, E., Redois, F., Fernandez-Gonzalez, M.,  
1998. *Ammonia Beccarii* and *Ammonia Tepida* (Foraminifera): Morphofunctional Arguments for  
878 Their Distinction. *Marine Micropaleontology*. 34, 235–244.

- 880 Debenay, J.-P., 1990. Recent foraminiferal assemblages and their distribution relative to environmental  
stress in the paralic environments of West Africa (Cape Timiris to Ebrie lagoon). *Journal of*  
882 *Foraminiferal Research*. 20, 267–282.
- 884 Donato, S.V., Reinhardt, E.G., Boyce, J.I., Rothaus, R., Vosmer, T., 2008. Identifying tsunami  
deposits using bivalve shell taphonomy. *Geology*. 36, 199–202.
- 886  
Donato, S.V., Reinhardt, E.G., Boyce, J.I., Pilarczyk, J.E., Jupp, B.P., 2009. Particle-Size Distribution  
888 of Inferred Tsunami Deposits in Sur Lagoon, Sultanate of Oman. *Marine Geology*. 257, 54–64.
- 890 El Hussain, I., Omira, R., Deif, A., Al-Hasbi, Z., Al-Rawas, G., Mohamad, A., Al-Jabri, K., Baptista,  
M.A., 2016. Probabilistic tsunami hazard assessment along Oman coast from submarines  
892 earthquakes in the Makran subduction zone. *Arabian Journal of Geosciences*. 9, 668.
- 894 Ellison, J. C., and Stoddart, D. R., 1991. Mangrove Ecosystem Collapse during Predicted Sea-Level  
Rise: Holocene Analogues and Implications. *Journal of Coastal Research*. 151–165.
- 896  
Erlandson, J. M., Braje, T. J., 2015. Coasting out of Africa: the potential of mangrove forests and marine  
898 habitats to facilitate human coastal expansion via the Southern Dispersal Route. *Quaternary*  
*International*. 382, 31–41.
- 900  
Evans, G., Kendall, V., Bush, P., Nelson, H., 1969. Stratigraphic and geologic history of the sebkha Abu  
902 Dhabi, Persian Gulf. *Sedimentology*. 12, 145–159.
- 904 Falkenroth, M., Schneider, B., Hoffmann, G., 2019. Beachrock as Sea-Level Indicator – A Case Study  
at the Coastline of Oman (Indian Ocean). *Quaternary Science Reviews*. 206, 81–98.
- 906

- 908 Fleitmann, D., Burns, S. J., Mangini, A., Mudelsee, M., Kramers, J., Villa, I., Neff, U., Al-Subbary,  
A.A., Buettner, A., Hippler, D., Matter, A., 2007. Holocene ITCZ and Indian Monsoon Dynamics  
Recorded in Stalagmites from Oman and Yemen (Socotra). *Quaternary Science Reviews*. 26, 170–  
910 88.
- 912 Fleitmann, D., Matter, A., 2009. The speleothem record of climate variability in Southern Arabia . *C R  
Geoscience*. 341, 633–642.
- 914
- 916 Fouache, E., Al-Maqbali, A., Beuzen-Waller, T., Desruelles, S., Giraud, J., Moaretis, D., Pavlopoulos,  
K., 2017. Geoarchaeological study of the Sur-Quriyat area (Oman), report of the 1rst season,  
Ministry of Culture and Heritage, Sultanate of Oman. Unpublished
- 918
- 920 Fournier, J., Bonnot-Courtois, C., Paris, R., Voltoire, O., Le Vot, M., 2012. *Analyses granulométriques,  
principes et méthodes*, CNRS (Eds), Dinard
- 922 Fritz, H.M., Blount, C.D., Al Busaidi, F.B., Al-Harty, A.H.M., 2010. Cyclone Gonu storm surge in  
Oman, *Estuarine. Coastal and Shelf Science*. 86, 102–106.
- 924
- 926 Giraud, J., 2009. The evolution of settlement patterns in the Eastern Oman from the Neolithic to the  
Early Bronze Age (6000-2000 B.C.). *Comptes Rendus Géosciences*. 341, 739–749.
- 928 Giraud, J., 2010. Early Bronze Age Graves and Graveyards in the Eastern Ja’alan (Sultanate of Oman):  
An Assessment of the Social Rules Working in the Evolution of a Funerary Landscape, in: Weeks,  
930 L. (Eds), *Death, Burial in Arabia and Beyond, Multidisciplinary perspectives*. Seminar for Arabian  
Studies Monographs, 10, BAR International Series. Archaeopress. Oxford, pp. 71–84.
- 932

- 934 Giesche, A., Staubwasser, M., Petrie, C. A., Hodell, D. A., 2018. Indian winter and summer monsoon  
strength over the 4.2 ka BP event in foraminifer isotope records from the Indus River delta in the  
Arabian Sea. *Climate of the Past*. 15, 73–90.
- 936
- 938 Haggag, M., Badry, H., 2012. Hydrometeorological Modeling Study of Tropical Cyclone Phet in the  
Arabian Sea in 2010. *Atmospheric and Climate Sciences*. 02, 174–90.
- 940 Hallmann, N. G., Camoin, A., Eisenhauer, A., Botella, G. A., Milne, C., Vella, E., Samankassou, E.,  
Pothin V., Dussouillez P., Fleury., J., Fietzke J., 2008. Ice Volume and Climate Changes from a  
942 6000 Year Sea-Level Record in French Polynesia. *Nature Communications*. 9. 285.
- 944 Hannss, C., 1998. Predominante features of the Quaternary relief development seawards of the Oman  
mountains as reflected in wadi and coastal terraces and other coastal features, in: Alsharhan, A.,  
946 Glennie K.W., Whittle, G.L., Kendall, C.G. (Eds), *Quaternary deserts and climatic change*.  
Balkema, Rotterdam
- 948
- Hannss, C., 1999. Quaternary wadi terraces in the river basin of Wadi Miglas and barriers beach near  
950 the outh of the Wadi Munayzif in relation to their general geomorphological and archaeological  
background (central Oman), in: Reihe, A. (Eds), *The capital area of Northern Oman. Teil II*.  
952 *Beihefte zum Tubinger Atlas des Vorderen Orients. Naturwissenschaften*
- 954 Hijma, M. P., Engelhart, S. E., Törnqvist, T. E., Horton, B. P., Hu, P., Hill, D. F., 2015. A Protocol for  
a Geological Sea-Level Database, in: Shennan, I., Long, A. J. and Horton, B.J. (Eds), *Handbook of*  
956 *Sea-Level Research*. Wiley Blackwell, pp. 536–553.
- 958 Hilbert, Y., Parton, A., Morley, M.W., Linnenlucke, L.P., Jacobs, Z., Clark-Balzan, L., Roberts, R.G.,  
Galletti, C.S., Schwenninger, J.-L., Rose, J.I., 2015. Terminal Pleistocene and Early Holocene  
960 archaeology and stratigraphy of the southern Nejd, Oman. *Quaternary International*. 382, 250–263.



- 962 Hoffmann, G., Reicherter, K., Wiatr, T., Grützner, C., Rausch T., 2013a. Block and Boulder  
Accumulations along the Coastline between Fins and Sur (Sultanate of Oman): Tsunamigenic  
964 Remains ?. *Natural Hazards*. 65, 851–73.
- 966 Hoffmann, G., Rupprechter, M., Mayrhofer, G., 2013b. Review of the Long-Term Coastal Evolution of  
North Oman – Subsidence versus uplift. *Zeitschrift Der Deutschen Gesellschaft Für*  
968 *Geowissenschaften*. 164, 237–252.
- 970 Hoffmann, G., Rupprechter, M., Al Balushi, N., Grützner, C., Reicherter, K., 2013c. The impact of the  
1945 Makran tsunami along the coastlines of the Arabian sea (Northern Indian Ocean)- a review.  
972 *Zeitschrift für Geomorphologie*. 57, 257–277.
- 974 Hoffmann, G., Grützner, C., Reicherter, K., Preusser, F., 2015. Geo-archaeological evidence for a  
Holocene extreme flooding event within Arabian Sea (Ras al Hadd, Oman). *Quaternary Science*  
976 *Reviews*. 113, 122–133.
- 978 Hoffmann, G., Schneider B., Mechernich, S., Falkenroth, M., Dunai T., Preusser, F. 2019. Quaternary  
uplift along a passive continental margin (Oman, Indian Ocean). *Geomorphology*. In Press  
980
- Horton, B.P., Edwards R. J., 2006. Quantifying holocene sea-level change using intertidal foraminifera:  
982 lessons from the British Isles. *Cushman Foundation for foraminiferal Research. Special*  
*Publication*. 40, 1–97.
- 984
- Jordan, B.R., 2008. Tsunamis of the arabian peninsula: a guide of historic events. *Science of tsunami*  
986 *hazards*. 1, 31–46.

- 988 Kaniewski, D., Marriner, N., Cheddadi, R., Guiot, J., Van Campo, E., 2018. The 4.2 ka BP event in the  
Levant. *Climate of the Past*. 14, 1529–1542.
- 990
- 992 Koster, B., Hoffmann, G., Grützner, C., Reicherter, K., 2014. Ground Penetrating Radar Facies of  
Inferred Tsunami Deposits on the Shores of the Arabian Sea (Northern Indian Ocean). *Marine  
Geology*. 351, 13–24.
- 994
- 996 Kusky, T., Robinson, C., El-Baz, F., 2005. Tertiary–Quaternary Faulting and Uplift in the Northern  
Oman Hajar Mountains. *Journal of the Geological Society*. 162, 871–888.
- 998 Lambeck, K., 1996. Shoreline Reconstructions for the Persian Gulf since the Last Glacial Maximum.  
*Earth and Planetary Science Letters*. 142, 43–57.
- 1000
- 1002 Lambeck, K. H. Rouby, H. A. Purcell, A., Sun, Y., Sambridge, M., 2014. Sea Level and Global Ice  
Volumes from the Last Glacial Maximum to the Holocene. *PNAS*. 111. 43, 15296–15303.
- 1004 Leckie, R.M., Olson H.C., 2003. Foraminifera as proxies for sea-level change on siliciclastic margins,  
in: Olson, H.C., and Leckie R.M. (Eds.), *Micropaleontologic Proxies for Sea-Level Change and  
Stratigraphic Discontinuities*. SEPM Special Publication no 75. Tulsa, Okla, pp. 5–19.
- 1006
- 1008 Lézine, A.M., Saliège, J. -F., Mathieu, R., Tagliatela, T. L., Méry, S., Charpentier, V., Cleuziou, S.,  
2002. Mangroves of Oman during the late Holocene: climatic implications and impact on human  
1010 settlements. *Vegetation History and Archaeobotany*. 11, 221–232.
- 1012 Lézine, A.M., Ivory, J. I., Braconnot, P., Marti, O., 2017. Timing of the southward retreat of the ITZC  
at the end of the Holocene Humid Period in Southern Arabia: Data model comparison. *Quaternary  
1014 Science reviews*. 64, 68–76.

- 1016 Krishna, K.M., 2009. Intensifying tropical cyclones over the North Indian Ocean during summer  
monsoon. *Global and planetary change*. 65, 12–16.
- 1018
- Le Métour, J., de Gramont, X., Villet, M., 1983. Geological map of Quryāt, Sultanate of Oman, Sheet  
1020 NF40-4D, scale 1:100 000. Ministry of Petroleum and Minerals, Directorate General of Minerals.
- 1022 Le Métour, J., 1992. Geological map of Muscat, Sultanate of Oman, Sheet NF 40-04, scale 1:250 000.  
Ministry of Petroleum and Minerals, Directorate General of Minerals.
- 1024
- Loreto, R., 2017. Note on the 2016 excavation season at BMH2 (Bimah, Sultanate of Oman).  
1026 *Newsletteri di Archaeologia CISA*. 8, 115–121.
- 1028 Morton, R.A., Gelfenbaum, G., Jaffe, B.E., 2007. Physical Criteria for Distinguishing Sandy Tsunami  
and Storm Deposits Using Modern Examples. *Sedimentary Geology*. 200, 184–207.
- 1030
- Munoz, O., Azzarà, V., Giscard, P-H, Hautefort, R., San Basilio, F., Saint-Jalm, L. 2017. First campaign  
1032 of survey and excavations at Shiyā (Sūr, Sultanate of Oman). *Proceedings of the Seminar for  
Arabian Studies*. 47, 185–192.
- 1034
- Murray, J.W., 1971. An atlas of British recent foraminiferids, Edition Heinemann educational books,  
1036 London, p. 244.
- 1038 Murty, T.S., El Sabh, M.I., 1984. Cyclones and strom surges in the Arabian Sea: a brief review. *Deep  
Sea Research Part A., Oceanographic Research papers*. 31, 665–670.
- 1040
- Parker, A.G., Goudie, A.S., Stokes, S., White, K., Hodson, M. J., Manning, M., Kennet, D., 2006. A  
1042 record of Holocene climate change from lake geochemical analyses in Southeastern Arabia,  
*Quaternary Research*. 66, 465–476.

1044

Parker, A.G., Preston, G.W., Parton, A., Walkington, H., Jardine, P.E., Leng, M.J., Hodson, M.J., 2016.

1046 Low latitude Holocene hydroclimate derived from lake sediments flux and geochemistry, journal  
of Quaternary Science, 31 (4), 286–299.

1048

Phillips, C.S., Wilkinson, T.J., 1979. Recently discovered shell middens near Quriyat. *Journal of Oman*

1050 *Studies*. 5, 107-110.

1052 Pilarczyk, J.E., Reinhardt, E.G., Boyce, J. I., Schwarcz, H.P., Donato, S.V., 2011. Assessing Surficial

Foraminiferal Distributions as an Overwash Indicator in Sur Lagoon, Sultanate of Oman. *Marine*

1054 *Micropaleontology*. 80, 62–73.

1056 Pilarczyk, J.E., Reinhardt, E.G., 2012. Testing Foraminiferal Taphonomy as a Tsunami Indicator in a

Shallow Arid System Lagoon: Sur, Sultanate of Oman. *Marine Geology*. 295-298, 128–136.

1058

Puga-Bernabéu, A., Aguirre, J., 2017. Contrasting Storm- versus Tsunami-Related Shell Beds in

1060 Shallow-Water Ramps. *Palaeogeography, Palaeoclimatology, Palaeoecology*. 471, 1-14.

1062 Purdue, L., Charbonnier, J., Régagnon, E., Calastrenc, C., Sagory, T., Virmoux, C., Crépy, M., Costa,

S., Benoist, A., 2019. Geoarchaeology of Holocene oasis formation, hydro-agricultural

1064 management and climate change in Masafi, southeast Arabia (UAE). *Quaternary Research*. 92,  
109–132.

1066

Reimer, P. J., Bard, E., Bayliss, A., Beck, J. W., Blackwell, P. J., Ramsey, C. B., Buck, C. E., Cheng,

1068 H., Edwards, R. L., Friedrich M., Grootes P. M., Guilderson T. P., Haffidason H., Hajdas I., Hatte

C., Heaton T. J., Hoffmann D. L., Hogg A. G., Hughen K. A., Kaiser K. F., Kromer B., Manning,

1070 S. W., Niu M., Reimer R. W., Richards D. A., Scott E. M., Southon J. R., Staff R. A., Turney C. S.

- 1072 M. and Van Der Plicht, J., 2013. Intcal13 and Marine13 radiocarbon age calibration curves 0-  
50,000 years cal BP. *Radiocarbon*. 55, 1869–1887.
- 1074 Rodriguez, M., Chamot-Rookes, N., Hébert, H., Fournier, M., Huchon, P., 2013. Owen ridge deep-water  
submarine landslides: implications for tsunami hazard along the Oman coast. *Natural Hazards and*  
1076 *Earth System Sciences*. 13, 417–424.
- 1078 Sanlaville, P., Dalongeville, R., Evin, J., Paskoff, R., 1987. Modification du tracé littoral sur la côte  
arabe du Golfe persique en relation avec l'archéologie. Déplacement des lignes de rivage en  
1080 Méditerranée. Paris CNRS, 211-222.
- 1082 Sanlaville, P., Dalongeville R., 2005. L'évolution des espaces littoraux du golfe Persique et du golfe  
d'Oman depuis la phase finale de la transgression postglaciaire. *Paléorient*. 31, 9–26.
- 1084 Sarawasti, P. K., 2002. Growth and habitat of some recent miliolid foraminifera: Palaeoecological  
1086 implications. *Current science*. 82, 81–84.
- 1088 Stokes, S., Bray, H. E., 2005. Late Pleistocene aeolian history of the Liwa region, Arabian Peninsula.  
Geological Society of America Bulletin. 117, 1466–1480
- 1090 Stuiver, M., Reimer, P. J., 1993. Extended 14 C data base and revised CALIB.3.0. 14 C age calibration  
1092 program. *Radiocarbon*. 35, 215–230.
- 1094 Tengberg, M., 2005. Les forêts de la mer. Exploitation et évolution des mangroves en Arabie Orientale  
du Néolithique à la période islamique. *Paléorient*. 31, 39–45.
- 1096 Uerpmann, M., 1992. Structuring the Late Stone Age of Southeast Arabia. *Arabian Archaeology and*  
1098 *Epigraphy*. 3, 65–109.

1100 Van Rampelbergh, M., Fleitmann, D., Verheyden, S., Cheng, H., Edwards, L., De Geest, P., De  
Vleeschouwer, D., Burns, S. J., Matter, A., Claeys, P., Keppens, E., 2013. Mid- to Late Holocene  
1102 Indian Ocean Monsoon Variability Recorded in Four Speleothems from Socotra Island, Yemen.  
Quaternary Science Reviews. 65, 129–42.

1104  
Wyns, R., Béchenec, F., Le Métour, J. Roger, J., 1992. Geological Map of the Tiwi Quadrangle,  
1106 Sultanate of Oman. Geoscience map, scale 1:100 000, Sheet 40-8B. Ministry of Petroleum and  
Minerals.

1108

## 1110 **Figures**

### 1112 **Figure 1. Overview of the area of study.**

Fig.1.a: Location of the Quriyat coastal plain, and of previous studies carried out in the region  
1114 and along the Quriyat-Sur coast

In fig. 1.b: From 1-10: studies mentioned in figure 11, ITZC positions are taken from Van  
1116 Rampelbergh *et al.* (2013)

In Fig. 1.c : Studies carried out in the Quriyat-Sur area : a) Study of tsunami boulders (Hoffmann  
1118 *et al.*, 2013a), and of coarse to fine grain overwash deposits (Koster *et al.*, 2014); b) Marine  
flooding event at 4450 cal. BP on the Early Bronze Age site HD-6, Ras al-Hadd (Hoffmann *et*  
1120 *al.*, 2015); c) In the Sur lagoon : study of the particle-size distribution of the 1945 tsunami  
deposits (Donato *et al.*, 2009), and study of the superficial foraminiferal distribution as an  
1122 overwash indicator (Pilarczyk *et al.*, 2011), localisation of the shell middens are taken from  
Biagi (1999).

1124 In fig. 1.d and 1.e: Satellite imagery of the Quriyat coastal plain, and localisation of sampling  
areas.

1126

**Fig. 2. Map of the archaeological sites from Muscat to Filim.** This map is a compilation of  
1128 data collected during surveys conducted by Jessica Giraud during her PhD and during the  
French geoarchaeological mission between Quriyat-Sur (2017), and surveys conducted by  
1130 Roland Besenval during the French-Italian archaeological program (2013-2015).

1132 **Fig. 3. Geomorphological map of the Quriyat coastal plain.** Geological data are extracted  
from Le Metour *et al.* (1983), alluvial terrace delimitation of the wadi Miglas and Munayzif are  
1134 adapted from Hannss (1999).

1136 **Fig. 4. Location of coring points in the different area of the Quriyat coastal plain:** a)  
Panoramic view of Quriyat coastal plain, b) dunes field, c) sebkha, d) drilling cores using a  
1138 Cobra vibracorer

1140 **Fig. 5. Trenches in the area of the Wadi Dayqah delta.**

1142 **Fig. 6. Distribution of molluscs and foraminifera according to specific marine/tidal  
environments.**

1144

**Fig. 7. Stratigraphic profile of the plain and main sedimentological units.**

1146

**Fig. 8. QT3 sedimentological, malacological and foraminiferal analyses.**

1148

**Fig. 9. QU4 sedimentological, malacological and foraminiferal analyses.**

1150

**Fig. 10. Schematic evolution of the Quriyat coastal plain suggested in this paper. The scale**

1152 **is not shown.**

1154 **Fig. 11. Comparison of the results obtained in Quriyat with regional terrestrial, marine  
and speleothems records in the United Arab Emirates and northern Oman.**

1156 a) Sea-level index points between Abu Dhabi (n°10 on Fig. 1) and Ja'alan (n°4 on Fig. 1); b)

The coastal evolution of Quriyat; c) The coastal evolution of Ja'alan (n°4); d) Distribution of

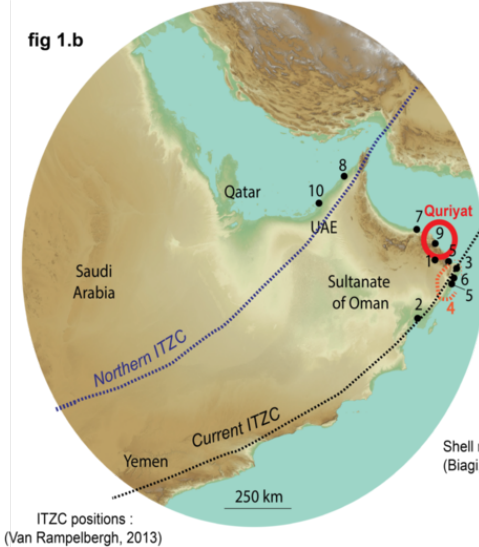
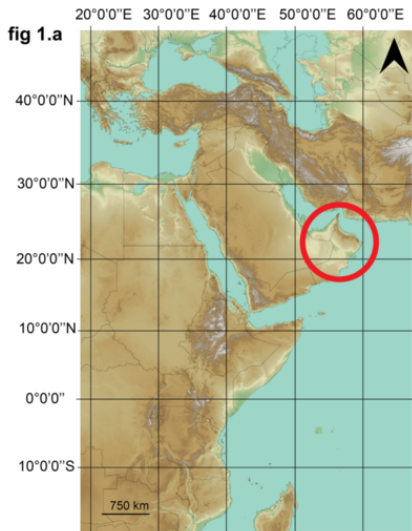
1158 *Avicennia* and *Rhizophora* in palynologic studies conducted at Kwar al Jaramah (n°3 on fig.1);

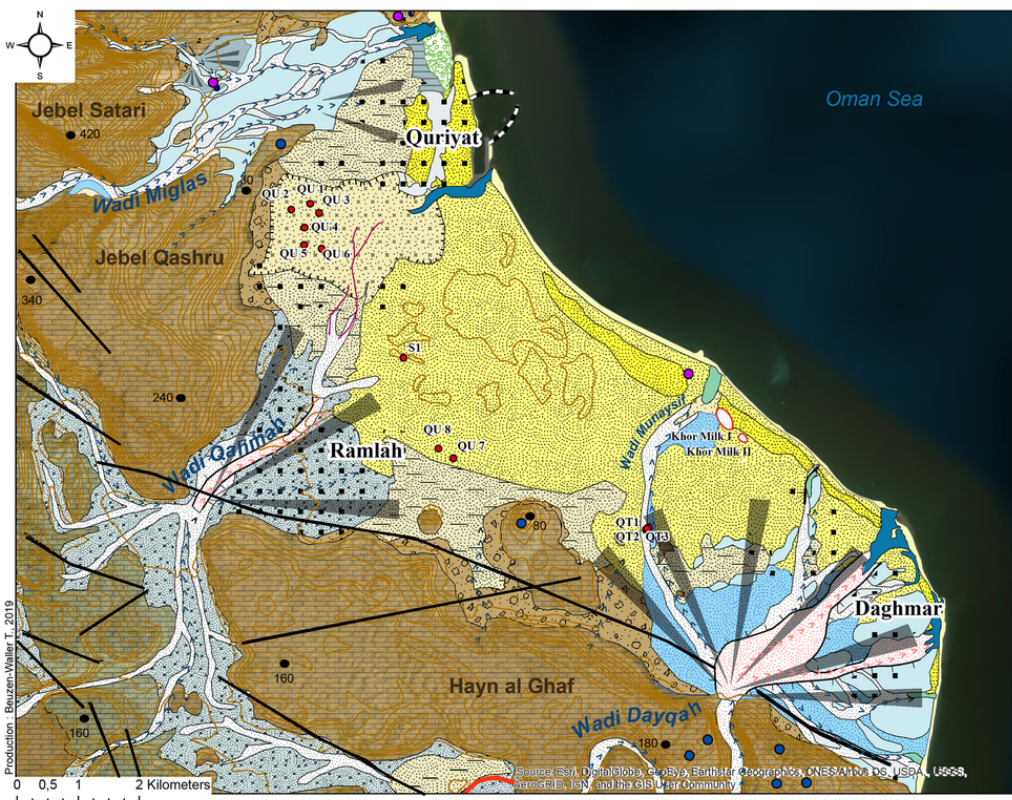
e) conducted at Filim (n°2 on Fig.1) in Lézine *et al.*, 2017; f) Pluvial signals studied on Hoti

1160 cave speleothems (n°1 on Fig.1) in Van Rampelberg *et al.*, 2013

1162







### Topography

- Contour lines (20m)
- Spot heights

### Lithology

- Tertiary limestones and conglomerates
- Secondary limestones, siltstone, conglomerates

### Tectonic

- Faults

### Slope dynamics

- Colluvial deposits, Slope debris

### Aeolian deposits

- Dunes field
- Coastal dune
- Beach dune

### Marine abrasion

- Inherited abrasion platform

### Lagoonal units

- Mangroves
- Closed lagoon
- Open lagoon
- Coastal sebkha (paleo-lagoon)

### Alluvial deposits

#### Active geomorphological units

- Wadi stream
- Kabhras deposits
- Exceptional floodplain
- Floodplain
- Unstable banks

#### Inherited geomorphological units

- Paleo-wadi
- Alluvial terraces T4
- Alluvial terraces T3
- Alluvial terraces T2
- Alluvial terraces T1
- Undetermined alluvial terraces
- Alluvial fans

### Anthropogenic units

#### Flood management

- Chenalized floodplain
- Chenalized wadi
- Dam
- Dikes

#### Coastal stabilization

- Seawall
- Embankments

#### Urbanisation

- Buildings

### Archaeological remains

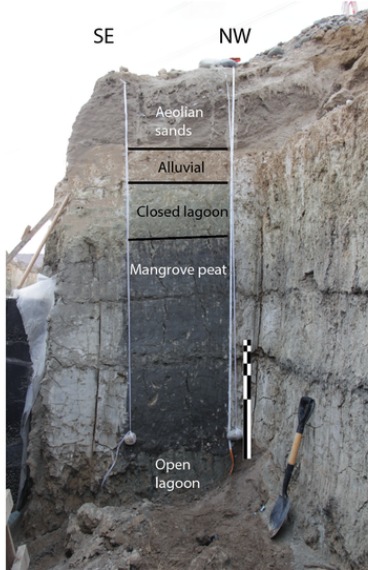
- Main shell midden (Khawr Milh)
- Archaeological sites
- Destroyed archaeological sites

### Samplings

- Coring and sounding

**A****B****C****D**

**A** QT1

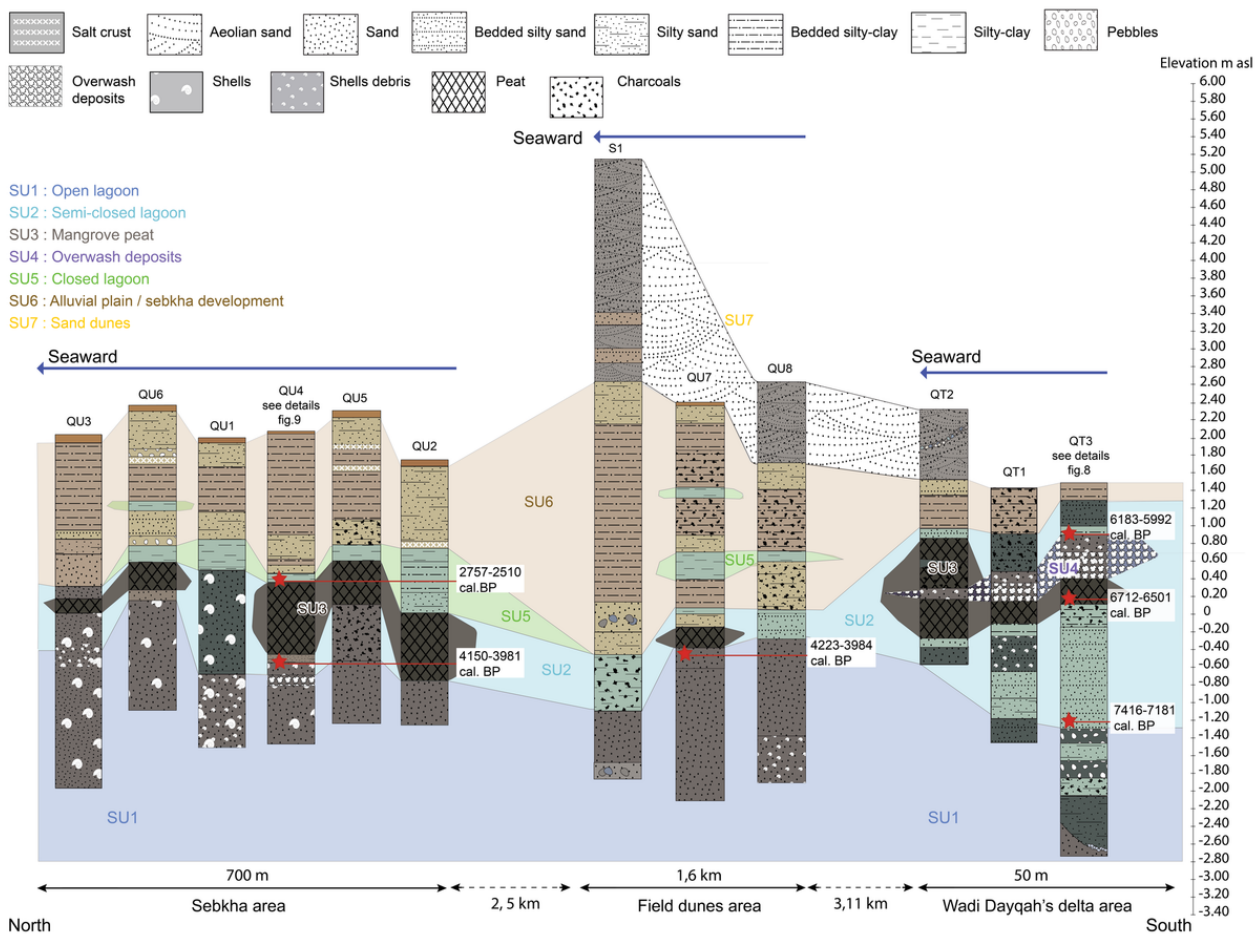


**B** QT2



**C** QT3





Salinity	Marine		Hyperhaline		Brackish		Euryhaline		
Foraminifera	<ul style="list-style-type: none"> <li>. <i>Amphistegina</i> sp.</li> <li>. <i>Cibicides pseudolobatus</i></li> <li>. <i>Textularia</i> sp.</li> <li>. <i>Spirillina</i> sp.</li> </ul>		<ul style="list-style-type: none"> <li>. <i>Ammonia parkinsoniana</i></li> <li>. <i>Miliolids</i></li> <li>. <i>Ammonia tepida</i></li> </ul>		<ul style="list-style-type: none"> <li>. <i>Brizalina striatula</i></li> <li>. <i>Elphidium Gerthi</i></li> <li>. <i>Elphidium craticulatum</i></li> <li>. <i>Elphidium advenum</i></li> </ul>		<ul style="list-style-type: none"> <li>. <i>Elphidium striatopunctatum</i></li> <li>. <i>Peneroplis planatus</i></li> <li>. <i>Cornuspira Schuktze</i></li> <li>. <i>Porosononion granosa</i></li> </ul>		<ul style="list-style-type: none"> <li>. <i>Ammonia tepida</i></li> </ul>
Tidal environments	Subtidal			Intertidal			Upper Intertidal		
Molluscs	<ul style="list-style-type: none"> <li>. <i>Ostrea</i></li> </ul>			<ul style="list-style-type: none"> <li>. <i>Nerita texilis</i></li> <li>. <i>Anadara</i></li> </ul>			<ul style="list-style-type: none"> <li>. <i>Ostrea</i></li> </ul>		
	<ul style="list-style-type: none"> <li>. <i>Nassarius castus</i></li> </ul>	<ul style="list-style-type: none"> <li>. <i>Rhinoclavis fasciata</i></li> </ul>	<ul style="list-style-type: none"> <li>. <i>Umbonium vestiarium</i></li> </ul>	<ul style="list-style-type: none"> <li>. <i>Rhinoclavis kochi</i></li> <li>. <i>Trochoidea</i></li> </ul>	<ul style="list-style-type: none"> <li>. <i>Potamides conicus</i></li> </ul>	<ul style="list-style-type: none"> <li>. <i>Terebralia palustris</i></li> </ul>	<ul style="list-style-type: none"> <li>. <i>Sacostrea cucullata</i></li> </ul>		
HAT									
LAT									
	Non-specific			Bay			Mangrove		
Shore habitats	Deep water zone	Shallow water zone		Sand	Under rocks	Mud		On rocks	

Elevation  
(m asl)

# QT3

2 sigma  
<sup>14</sup>C age  
(cal. BP)

Caliber

D50

Mode

Unprocessed  
sediments

Inorganic  
sediments

Inorganic and  
decarbonated  
sediments

Foraminiferal  
assemblages

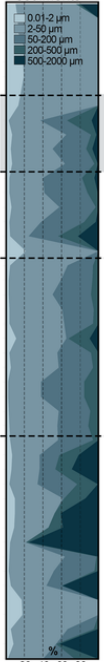
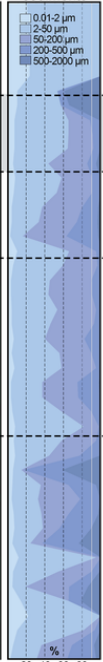
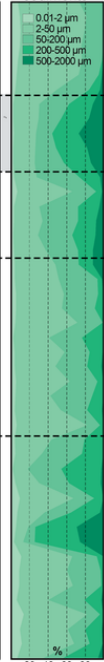
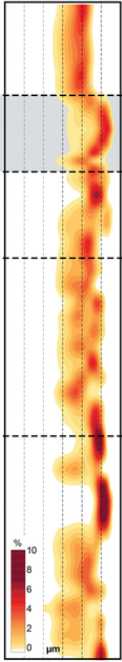
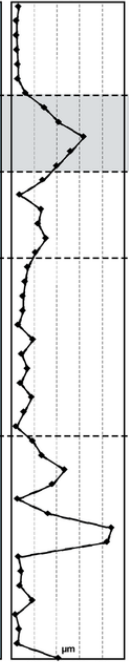
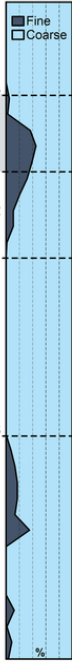
Malacological  
identification

Stratigra-  
phic units

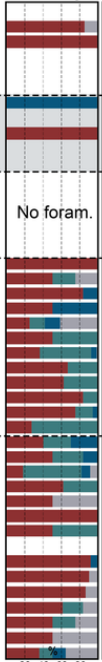
1.6  
1.4  
1.2  
1  
0.8  
0.6  
0.4  
0.2  
0  
-0.2  
-0.4  
-0.6  
-0.8  
-1  
-1.2  
-1.4  
-1.6  
-1.8  
-2  
-2.2  
-2.4  
-2.6  
-2.8



★ 5992-6183  
★ 6501-6712  
★ 7183-7416

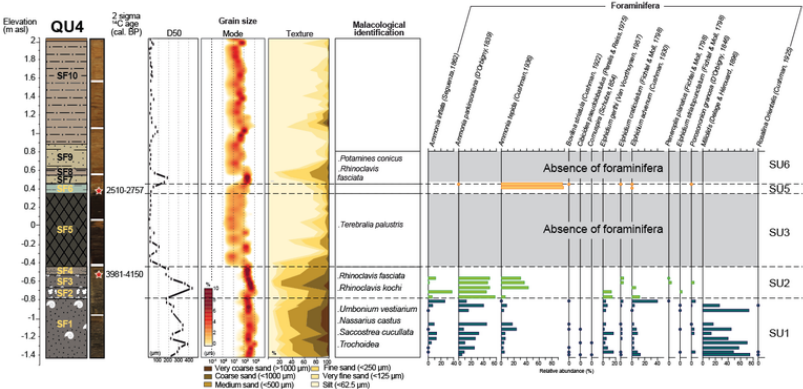


Hypersaline species  
Brackish species  
Marine species  
Undifferentiated



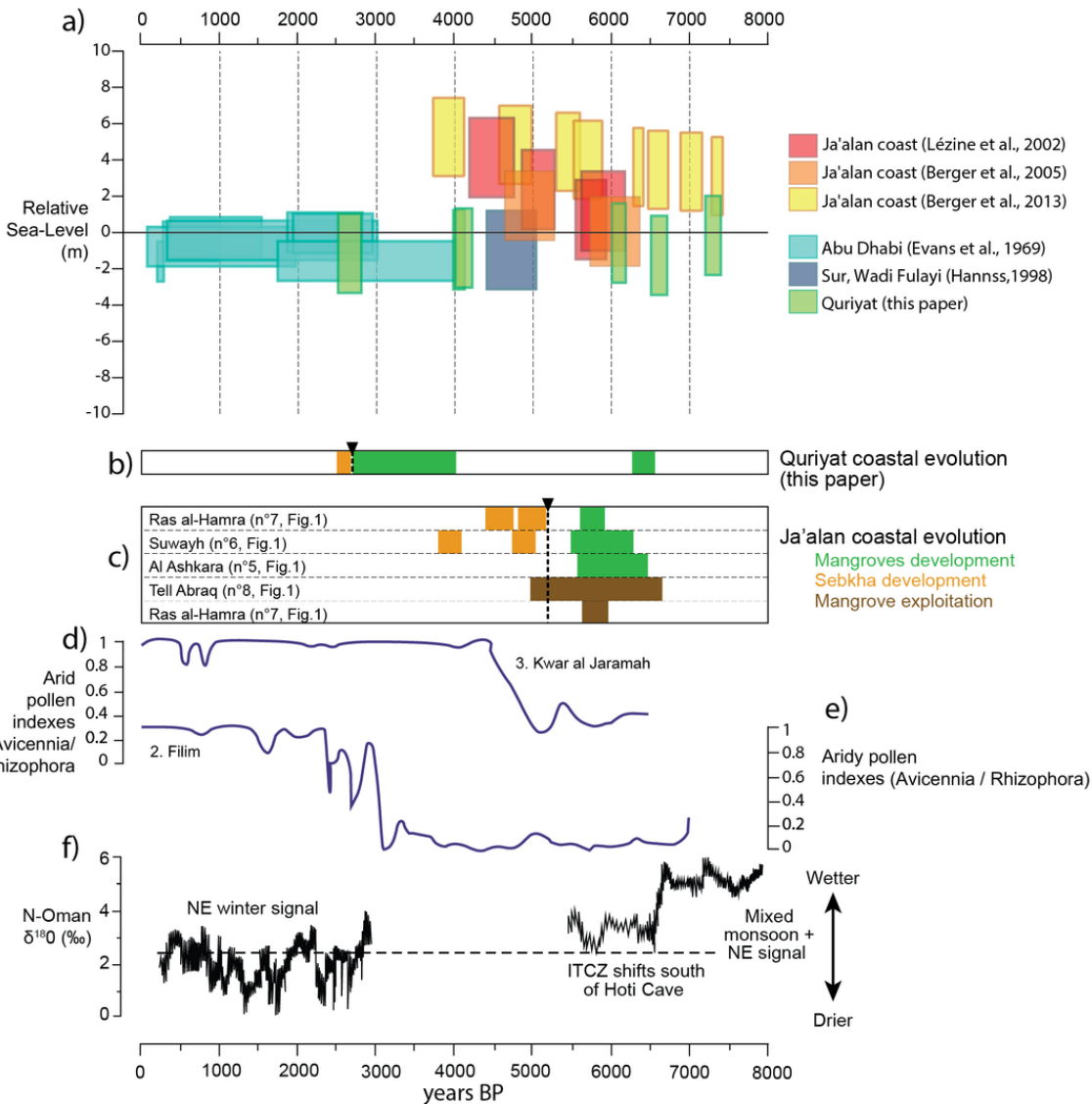
*Ostrea sp.*  
*Anadara sp.*  
*Nerita textilis*  
*Terebralia palustris*

SU5  
SU4  
SU3  
SU2  
SU1





years BP



Samples ID	Lab number	Origin	Elevation (related to mid-tide level)	Material	Conventional radiocarbon Age	Calib. 2 sigma BP	Calib. 2 sigma BC	Source	Country
QU4-E167	Beta - 401301	Core QU4 -Sebkha	+ 30 cm	Charcoal	2570 +/- 30 BP	2757-2510	808 -561	This study	Oman
QU4-E246	Beta - 401302	Core QU4 -Sebkha	- 50 cm	Charcoal	3720 +/- 30 BP	4150-3981	2201-2032	This study	Oman
QU7 C6 E288	Beta - 421589	Core QU7-Dune	- 60 cm	Wood	3740 +/- 30 BP	4223-3984	2074-2035	This study	Oman
QT3 E150	Beta - 469157	Trench QT3-Delta	- 130 cm	Charcoal	6360 +/- 30 BP	7416-7183	5467-5234	This study	Oman
QT3 E303	Beta - 469158	Trench QT3-Delta	+ 20 cm	Charcoal	5810 +/- 30 BP	6712-6501	4728-4552	This study	Oman
QT3 E 370-380	Beta - 471004	Trench QT3-Delta	+ 90 cm	Charcoal	5300 +/- 30 BP	6183-5992	4234-4043	This study	Oman

Name	Type	Area	X	Y	Elevation (m asl)
QU1	Core	Sebkha	694493	2572834	1.99
QU2	Core	Sebkha	694205	2572743	1.75
QU3	Core	Sebkha	694627	2572697	2.02
QU4	Core	Sebkha	694407	2572478	2.04
QU5	Core	Sebkha	694407	2572216	2.27
QU6	Core	Sebkha	694673	2572165	2.36
QU7	Core	Dunes	696475	2569170	2.40
QU8	Core	Dunes	696705	2569190	2.63
S1	Section	Dunes	695995	2570525	5.91
QT1	Trench	Wadi Dayqah area	699621	2568038	2.32
QT2	Trench	Wadi Dayqah area	699659	2568059	1.45
QT3	Trench	Wadi Dayqah area	699611	2568023	1.53